



SCHOOL of
GRADUATE STUDIES
EAST TENNESSEE STATE UNIVERSITY

East Tennessee State University
Digital Commons @ East
Tennessee State University

Electronic Theses and Dissertations

Student Works

8-2016

Silver-Polymer Nanocomposites

Anita N. Paul

East Tennessee State University

Follow this and additional works at: <https://dc.etsu.edu/etd>



Part of the [Organic Chemistry Commons](#)

Recommended Citation

Paul, Anita N., "Silver-Polymer Nanocomposites" (2016). *Electronic Theses and Dissertations*. Paper 3077. <https://dc.etsu.edu/etd/3077>

This Thesis - Open Access is brought to you for free and open access by the Student Works at Digital Commons @ East Tennessee State University. It has been accepted for inclusion in Electronic Theses and Dissertations by an authorized administrator of Digital Commons @ East Tennessee State University. For more information, please contact digilib@etsu.edu.

Silver-Polymer Nanocomposites

A thesis
presented to
the faculty of the Department of Chemistry
East Tennessee State University

In partial fulfillment
of the requirements for the degree
Master of Science in Chemistry

by
Anita Paul
August 2016

Dr. Aleksey Vasiliev, PhD, Chair

Dr. Greg Bishop, PhD

Dr. Hua Mei, PhD

Keywords: Silver nanoparticles, Nanocomposites, Thiolation, Condensation, Colloidal dispersion, Polymers, Coating, Dispersibility, Bactericide.

ABSTRACT

Silver-Polymer Nanocomposites

by

Anita Paul

The objective of this research was the development of an efficient method for the preparation of silver-polymer nanocomposites containing finely dispersed silver nanoparticles. The surface of nanosilver was functionalized by thiolation with 2-aminoethanethiol. Amino-modified nanosilver was covalently bonded to polyacrylic acid, an acid terminated polylactic acid, ester terminated poly(D,L-lactide-co-glycolide) and acid terminated poly(D,L-lactide-co-glycolide) by carbodiimide method using diisopropyl carbodiimide. Esterification of the carboxyl groups of Ag-polyacrylic acid by hydrochloric acid in methanol resulted in the dispersion of Ag nanoparticles in the polymer. The reaction of the ester terminated polymer with the functionalized nanosilver was due to the aminolysis of the ester bond in the polymer chain by the surface amino groups. Silver-polymer nanocomposites obtained with acid terminated polymers contained highly dispersed nanosilver in the polymer as compared to the ester terminated polymer. The attained biodegradable nanocomposites confirmed X-ray contrast and bactericidal properties, which could be eventually used for biomedical applications.

DEDICATION

This thesis is dedicated to my Lord and Savior Jesus Christ who has given me the wisdom to conduct research and complete this thesis adequately.

I also dedicate this thesis to my wonderful husband, Paul, and my delightful children, Natania, Nathan, and Natadria, for their love and inspiration.

ACKNOWLEDGEMENTS

As I write this thank you note — a finishing touch to my thesis, my heart is filled with gratitude toward all who have played a vital role in my life and have made this desire a reality.

I thank God my Savior for His faithfulness, amazing grace, unfailing love over me, and for giving me the opportunity to study at East Tennessee State University (ETSU). My gratitude goes to my dear husband, Paul, and my precious children, Natania, Nathan, and Natadria, for their understanding, reassurance, and steadfast support. Words cannot express how grateful I am to my late sweet mom for cheering me during my studies. I am thankful to my dad for his support and also instilling in me the value of education right from my childhood days. My heartfelt thanks go also to my loving mother-in-law and my late father-in-law for their encouragement.

I would like to express my appreciation to Dr. Aleksey Vasiliev, my research advisor, whose proficiency and knowledge have added value to my research. I thank him very much for his valuable guidance, counsel, and insightful comments. Thanks to my committee members Dr. Greg Bishop and Dr. Hua Mei for their advice and thought provoking questions. Dr. Reza Mohseni's assistance toward nuclear magnetic resonance spectroscopy and atomic absorption spectroscopy was incredible and I am very thankful to him for his help. My gratefulness also to Mr. Jordan Ellison, Mr. Greg Wykoff, and Mr. Jonathan Bailey for their assistance in the research.

I am thankful to Dr. Yu Gomza for his aid with the X-ray diffraction analysis, Dr. Leonid Golovko for his help in the transmission electron microscopy images, Dr. Fred Hossler from the ETSU department of Biomedical Sciences for his guidance in the scanning electron microscopy images, Ms. Victoria Leonard from Wellmont Hospital, Johnson City for taking the

X-ray images and Dr. Ekaterina Kaverina from ETSU department of Biological Sciences for her help in the toxicological study.

I am very appreciative of Dr. Scott Kirkby's intriguing questions and comments during research scrum. These questions were extremely beneficial to me. My gratitude also goes to Dr. Cassandra Eagle, Ms. Jillian Quirante, Mr. Ryan Alexander, Mr. Justin Pritchard, ETSU Chemistry professors, and graduate students for their motivation which enabled me to have a remarkable experience at ETSU. Last but not the least, I am immensely grateful to many special friends who have come by my side and have cheered me up. Their friendship is unforgettable.

Thanks once again to all of you for making this journey a memorable and meaningful one.

TABLE OF CONTENTS

	Page
ABSTRACT	2
DEDICATION	3
ACKNOWLEDGEMENTS	4
LIST OF TABLES	9
LIST OF FIGURES	10
Chapter	
1. INTRODUCTION	12
Nanomaterials	12
Silver Nanoparticles	15
Synthesis by Chemical Reduction	15
Photochemical Method	15
Properties of Silver Nanoparticles	16
Surface Plasmon Resonance	16
Hydrophilicity of Silver Surface	17
Bactericidal Properties	18
Applications of Silver Nanoparticles	20
Silver-Polymer Nanocomposites.....	21
In situ Polymerization	21
Ex situ Polymerization	22

Applications of Silver-Polymer Nanocomposites	23
Optical Applications	23
Electrical Applications	23
Antimicrobial Applications	23
Modification of Silver Surface by Thiolation	25
Objective	27
2. EXPERIMENTAL METHODS	28
Chemicals and Reagents	28
Synthetic Procedures	29
Thiolation of Silver Surface	29
Synthesis of Silver-Polymer Nanocomposites	30
Characterization	32
Atomic Absorption Spectroscopy	32
Determination of Polymer Contents by Weight Method	33
NMR Spectroscopy	33
X-ray Diffraction Analysis.....	33
Transmission Electron Microscopy	34
Fourier Transform Infrared Spectroscopy	34
Ultraviolet-Visible Spectroscopy	34
Scanning Electron Microscopy	34
X-ray Imaging	34
Microbiological Study	35
3. RESULTS AND DISCUSSION	36

Ag-PAA Nanocomposites	36
Composition	36
Fourier Transform Infrared Spectroscopy	37
Nuclear Magnetic Resonance Spectroscopy	38
Transmission Electron Microscopy	39
X-ray Diffraction Spectrometry	39
Ag-PLA and Ag-PLGA Nanocomposites	40
Composition	40
FT-IR Spectra	41
UV-Vis Spectra	42
SEM	42
X-ray Images	44
Toxicological Effect against E. coli	44
Discussion	45
Ag-PAA Nanocomposites	45
Ag-PLA and Ag-PLGA Nanocomposites	46
Conclusions	49
REFERENCES	51
VITA	60

LIST OF TABLES

Table	Page
1. Chemicals	28
2. Contents of Silver in Materials	41

LIST OF FIGURES

Figure	Page
1. Slide that Faraday used in his lecture in gold sols	12
2. A simple model of the surface area of nanoparticles	13
3. Surface plasmon resonance	17
4. Interaction of E. coli, typhus, P. aeruginosa and V. cholera with silver nanoparticles	19
5. Formation of chitosan-PVA silver nanoparticles film and curcumin loaded chitosan nanoparticles film	21
6. Ex situ method	22
7. Self-assembled monolayer	26
8. Thiolation of silver surface	30
9. Synthesis of Ag-PMA (1)	31
10. Scheme of the synthesis of nanocomposites 2-4	32
11. Agglomeration and deagglomeration of silver nanoparticles	36
12. IR spectrum of Polyacrylic acid.....	37
13. FT-IR spectrum of Ag-PMA	37
14. NMR Spectra of Ag-PMA	38
15. TEM image of Ag-PMA	39
16. XRD Spectrum of Ag-PMA	40
17. FT-IR spectra	42
18. UV-vis spectra	43
19. SEM images	43
20. X-ray images	44

21. Antibacterial activity of Pure Polymers	44
22. Surface Aminolysis of Ag-PLGA	47

CHAPTER 1

INTRODUCTION

Nanomaterials

Nanotechnology alludes to the field of science and engineering and is exclusively allocated to nanomaterials having dimensions in the order of 100 nm or less. The birth of nanoscience could be attributed to Michael Faraday who had reported in 1857 that the intense red color of certain stained glass was derived from small particles of gold. He had also indicated that the variation in the size of gold particles gave rise to a variety of resultant colors¹ (Fig. 1).



Figure 1: Slide that Faraday used in his lecture in gold sols²

Nanomaterials are of great importance in the scientific world due to the materials being a bridge between bulk materials and isolated atoms and molecules. The nanoscale materials are not made up of single atoms but clusters of atoms and molecules, for example, 3.5 atoms of gold or 8 hydrogen atoms lined up in a row are nearly 1 nanometer long. The mass of a nanomaterial is exceedingly small and its gravitational force is insignificant due to the small size of the particle.³ The fraction of atoms at the surface of the nanoparticles are increased due to the large surface to volume ratio. Consider a cube with edges 1 cm in length – divided into cubes with edges 1 mm in length – divided into cubes with edges 1 nm in length. Each time the 1cm cube is divided into smaller cubes, the volume of cubes remains constant whereas the surface area increases

significantly. The surface area of 1 cube is 0.0006 m^2 whereas the surface area of 10^{21} nanocubes is 6000 m^2 . This is illustrated in the diagram of cubes in Fig. 2.⁴

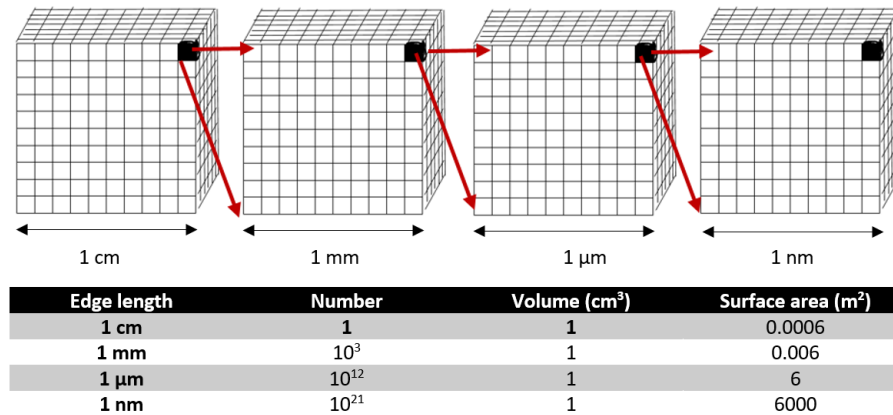


Figure 2: A simple model of the surface area of nanoparticles Adapted from ⁴

Nanomaterials have various properties as compared to bulk metals. They differ in quantum effects, optical properties, catalytic properties, melting point and mechanical properties.

a) Quantum Effects. In bulk metal, as the atoms come closer, the lower and the higher energy bands overlap forming a continuous band of energy levels with the electrons moving freely. But as the particle size decreases below the Bohr radius of the semiconductor material, the electron becomes more confined in the particle leading to an increase in the band gap energy. The valence band and the conduction band breaks into quantized energy levels resulting in the formation of nanoparticles of various sizes. This band gap emission is observed to shift leading to a red emission for the largest particles and blue emission for the smallest particles.⁵

b) Optical Properties. In a bulk metal, the electrons are excited to a higher energy level as the electrons on the surface of the metal absorb the wavelength of incident light. These excited electrons then return to the lower energy level emitting a photon of light at the same wavelength. This causes a metallic glow and good reflectivity in silver metal due to the

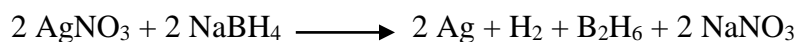
inability of the absorption of light by the electrons bound to atoms in the metal. At the nanoscale level, depending on the size of the nanoparticles, the electron clouds will resonate with a particular wavelength of light and absorb that wavelength causing the color of the nanoparticles to change.⁶ This characteristic color change is due to the collective oscillation of the electrons in the conduction band known as the surface plasmon resonance.⁵

- c) Catalytic Properties. Since metal nanoparticles have a higher surface area, there is an increased catalytic activity on the surface. Gold is an inert material and it does not tarnish. It is also resistant to chemical attack. However, when bulk gold is broken down to nano size it can act as a catalyst and oxidize carbon monoxide. The exposed atoms at the surface of a gold nanomaterial are more reactive than gold atoms in the bulk form and this is the cause of the gold nanoparticles to act as a catalyst in chemical reactions.⁶
- d) Melting Point. A bulk gold melts at a specific melting temperature despite melting a bracelet or a big bar of gold whereas a nanomaterial melts at an extremely low temperature. Due to the exposure of number of atoms on the surface of a nanoparticle, heat can break the bond between these atoms at a low temperature and cause a decrease in the melting point of the nanoparticle.⁶ It was observed that the melting point of a 10 nm particle dropped below that of a bulk gold metal (1064 °C) due to the reduction in its particle size.⁷
- e) Mechanical Properties. The tensile strength and elasticity of a nanomaterial are higher than a bulk metal and this is visible in the case of silicon nanowires and bulk silicon. Silicon nanowires are resilient and can be deformed very easily whereas bulk silicon is very brittle and has less deformability.⁸

Silver Nanoparticles

Synthesis by Chemical Reduction

The reduction is the gain of electrons or a decrease in oxidation state by a molecule, atom or ion. In a chemical reaction, an oxidizing agent gains electrons and is itself reduced whereas a reducing agent loses electrons and is oxidized. The reduction method is well known for the preparation of silver nanoparticles which are to be used as stable dispersions in organic solvents. This is done by the reduction of silver ions. Reducing agents such as sodium borohydride, hydrazine and formaldehyde can be said to reduce silver salts such as silver acetate, silver nitrate, to produce nano silver particles. Zielinska et al. prepared silver nanoparticles by the addition of silver precursor (silver nitrate) dropwise into an aqueous solution of sodium borohydride resulting in the formation of Ag nanoparticles. Sodium borohydride was also used for stabilizing the growing silver nanoparticles by providing a particle surface charge.⁹ Sodium borohydride on reaction with AgNO₃, formed a light yellow solution, which then changed to violet color and ultimately grayish color Ag nanoparticles.¹⁰

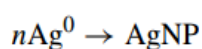
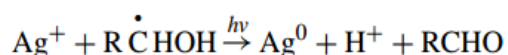
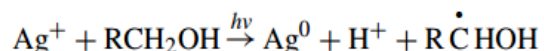
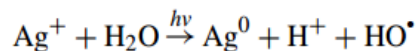


Also, silver nanoparticles were prepared by mixing silver nitrate as a precursor with sodium dodecyl sulfate, sodium citrate, and hydrazine hydrate. Sodium citrate and sodium dodecyl sulfate were used as stabilizing agents to stabilize the nanoparticles against aggregation by steric repulsion and hydrazine hydrate was used as a reducing agent.¹¹

Photochemical Method

This method is based on the reduction of the metal cation Mⁿ⁺ to M⁰ by light assisted methods. Here the mechanism is based on the addition of one or more electrons to a photoexcited species. Silver perchlorate (AgClO₄) in aqueous and alcoholic solution was subjected to photoreduction

by irradiation with UV-light at 254 nm. This photochemical reaction was based on the electron transfer from a solvent molecule to the electronically excited state of Ag^+ to form Ag^0 .



UV excitation is usually required in most instances since the metal cations and / or the metal salts absorb only in this region. It is advantageous as harsh conditions such as increased temperatures are avoidable resulting in easier control of shape and size of AgNP.¹²

Properties of silver nanoparticles

Surface Plasmon Resonance

Surface plasmon resonance (SPR) is the fundamental cause of the optical properties of silver nanoparticles. Surface plasmon resonance occurs when light incident on the nanoparticles is resonant with the collective oscillation of free conduction band electrons of the nanoparticle. This is dependent on the nanoparticle size, shape, inter-particle distance, dielectric properties of the nanoparticle and the surrounding medium.¹³ It was observed that certain wavelengths of light could cause the conduction electrons of the nanoparticle to oscillate and when the resonances were excited, the absorption and scattering intensities were found to be higher than similar sized non-plasmonic particles (Fig. 3).

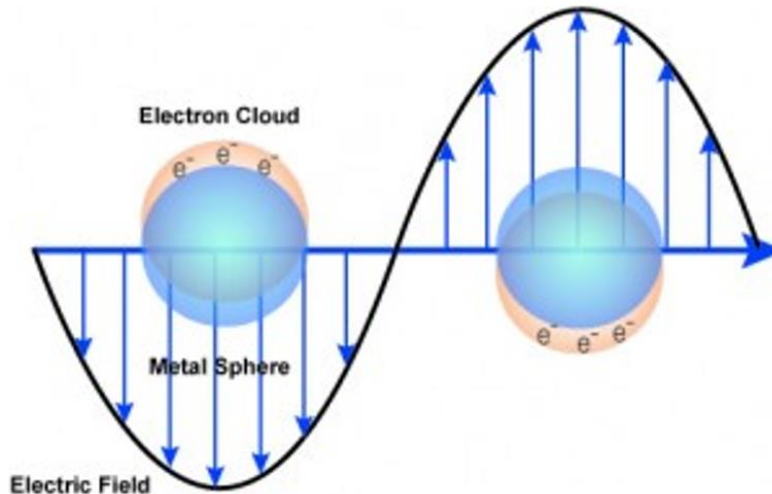


Figure 3: Surface plasmon resonance¹⁴

The absorption and scattering properties could be adjusted by regulating the particle size, shape and the local refractive index near the particle surface. It was noticed that small sized nanospheres absorbed light and had peaks toward shorter wavelength while large spheres had increased scattering and had peaks toward longer wavelength. This phenomenon was also perceived with the increase in the refractive index near the nanoparticle surface. There was also a noticeable change in the surface plasmon resonance of agglomerated silver nanoparticles with the shift toward lower energies (red shift). The aggregated silver nanoparticles looked gray in color whereas the deagglomerated particles appeared yellow in color.¹⁵

Hydrophilicity of Silver Surface

Hydrophilic molecules are those that form ionic or hydrogen bond with the water molecule. Silver nanoparticles, when exposed to the environmental surroundings, undergo oxidation and are contaminated. These metal oxides are susceptible to hydrogen bonding with the moisture in the environment. The bonds are strong and hence, water completely prefers to wet the surface¹⁶ making silver more hydrophilic.

Bactericidal Properties

Silver nanoparticles can affect the viability of bacteria through four distinct mechanisms.

- a) The permeability of the nanoparticles inside the cell membrane of the bacteria. The nanoparticles were visible not only on the surface of the cell membrane but also inside the cell membrane of the bacteria. When silver binds to the enzymes located on the bacterial plasma membrane, the enzymes change shape causing the enzymes to be activated. Due to the activation of the enzymes, silver nanoparticles easily permeate the membrane and enter into the bacterial cell. This prevents the nutrients from entering into the bacterial cell causing bacterial cell death (Fig. 4).¹⁷
- b) Binding of the nanoparticles to sulfur containing proteins of the cell membrane of the bacteria. After binding to the sulfur containing proteins, silver easily enters into the cell. Once inside the cell, silver reacts with other sulfur-containing proteins in the cell as well as sugar-phosphate backbone of DNA. Since bacterial cells do not contain membrane-bound organelles, silver nanoparticles can easily enter into the DNA of the bacteria to inhibit the cell division causing bacterial cell death.¹⁷
- c) Electrostatic interaction of the nanoparticles with the bacteria. The surface of the bacteria is negatively charged due to the dissociation of an excess number of carboxylic and other groups in the membrane. The nanoparticles immobilized in the carbon matrix experiences friction of the nanoparticles due to the movement inside the matrix and produces a charge on the surface. This causes an electrostatic interaction of the nanoparticles with the bacteria which may lead to the possibility of the bacteria's inhibition.¹⁷

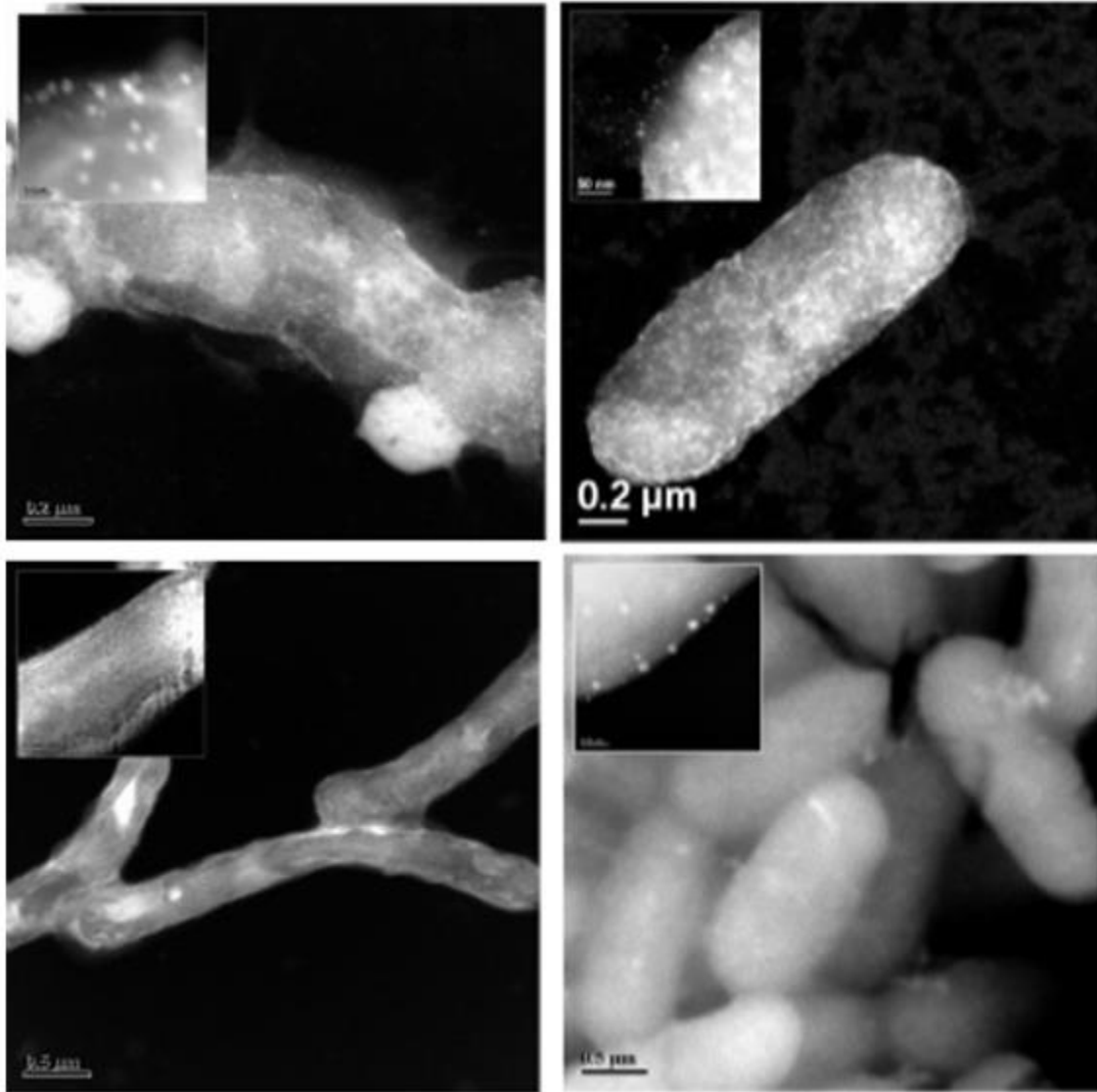


Figure 4: Interaction of *E. coli*, typhus, *P. aeruginosa* and *V. cholera* with silver nanoparticles¹⁷

- d) The presence of silver ions. The release of silver ions by the oxidation of nanoparticles upon contact with proteins in the cytoplasm liberates Ag^+ ions thus increasing the toxicity and thereby playing a major role in the bactericidal effect of silver nanoparticles. Ionic silver interacts with the enzymes of the bacterial respiratory chain causing the death of the cell.¹⁸ It has also been proved that silver ions cause the DNA to lose its replication ability and therefore cause the inhibition of the bacteria.¹⁷

The ability of silver nanoparticles to penetrate into the human cell depends on their size. The smaller nanoparticles have stronger activity because of the increased surface to volume ratio. It has been reported by Zhang et al. that smaller AgNPs (5 nm to 28 nm) confined in the mitochondrial complex can produce large amounts of hydrogen peroxide and induce considerable inflammasome formation because they can cause intense leakage of cathepsins from lysosomes. This can also cause more efflux of intracellular K^+ and produce a vast amount of superoxide. It has also been validated that silver nanoparticles and ionic silver can cause DNA damage from oxidation stress.¹⁹

Applications of Silver Nanoparticles

The antibacterial effect of silver nanoparticles enables their use in the food industry as food storage containers, fresh food bags, disinfecting sprays, deodorants and other cosmetics. Spherical silver nanomaterials are found in antimicrobial plant sprays and are used to protect plants from bacteria, virus, fungi, and algae. They are utilized in wound dressings, dental hygiene, treatment of eye conditions, vascular prosthesis, catheters, and orthopedics. Various forms of nanosilver have been used in the field of electronics (transparent conducting films, transparent electrodes for touch screens). Solar cells use these nanoparticles to generate power and also to re-charge the batteries to supply power in the night.²⁰ AgNP with localized surface plasmon resonance shift is used as a biosensor in detecting p53 protein levels in samples from head and neck squamous cell carcinoma (HNSCC) patients.²¹ Due to quantum confinement, semiconductor quantum supralattices (regular arrays of monodispersed semiconductor quantum dots) represented by a sodalite lattice containing silver halide [(8Ag,2X-SOD), where SOD = $Si_6Al_6O_{24}$] can be used for non-linear optical materials like second harmonic generator.²²

Silver-Polymer Nanocomposites

Nanocomposites are multiphase solid materials where one of the phases has dimensions of less than 100 nm. Silver nanoparticles can be incorporated into the polymer matrix to enhance its performance. Polymer functions not only as an excellent host for embedding nanoparticles but also for terminating the growth of the particles by controlling their nucleation.²³

Silver-polymer nanocomposites can be obtained using two main approaches.

In situ Polymerization

In the in situ method, the silver nanoparticles are produced inside a polymer by chemical reduction of a metallic precursor which is dissolved in the polymer. The reduction potential is from Ag^+ to Ag^0 and it uses several reducing agents like sodium borohydride, hydrazine etc. Curcumin-loaded chitosan-PVA silver nanoparticles film (CCPSNP) was prepared by the addition of AgNO_3 to chitosan solution resulting in the formation of AgNP solution to which, poly(vinyl alcohol), glutaraldehyde (a crosslinker) and curcumin solution were added. Here the Ag^+ ions were reduced to Ag nanoparticles on irradiation with sunlight (Fig. 5).²⁴

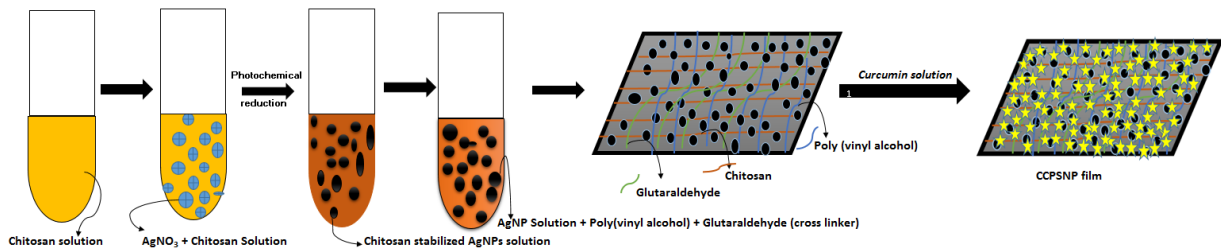


Figure 5: Formation of chitosan-PVA silver nanoparticles film and curcumin-loaded chitosan nanoparticles film Adapted from²⁴

Porel and his group synthesized Ag-PVA film by mixing an aqueous solution of AgNO_3 and poly(vinyl alcohol) (PVA) wherein the precursor Ag ions from AgNO_3 was reduced by the

hydroxyl groups of the PVA macromolecule.²⁵ Ag-polyaniline nanocomposite was prepared by mixing aniline and silver nitrate as precursor after well rinsing with nitric acid.²⁶

Ex situ Polymerization

In the ex situ method, silver nanoparticles are formed first and then dispersed into a polymer matrix. The nanoparticles that are formed possess higher dispersibility in the polymer and have long term stability against aggregation. Dispersion of nanoparticles was obtained by sonication²⁷ (Fig. 6).

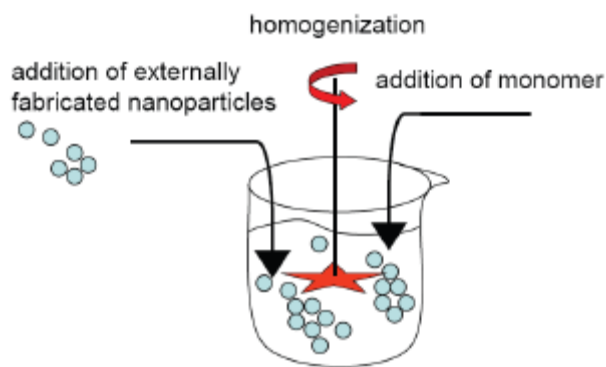


Figure 6: Ex situ method²⁸

Ag-poly(ethylene-co-propylene)-p-benzoquinone polymer matrix was prepared by dispersing Ag nanoparticles and para-benzoquinone in a toluene solution containing ethylene-co-propylene.²⁹

Fortunati et al. produced Ag-PLGA nanocomposites film by mixing PLGA (dissolved in chloroform) with Ag nanoparticles (dispersed in chloroform).³⁰ Thin nanocomposites films, containing silver nanocrystal in a polystyrene matrix, were prepared by sonicating silver nanoparticles with toluene and polystyrene for even dispersion of the nanoparticles.³¹

Ag-poly(methyl methacrylate)-poly(ethylene terephthalate) (Ag-PMMA-PET) film was prepared by electron beam evaporation of silver with PMMA-PET structure.³² Zeng et al. formed Ag-polystyrene film by homogeneous dispersion of Ag nanoparticles in polystyrene solution with chloroform as solvent utilizing ultrasonic agitation.³³ Polyurethane nanocomposites were

prepared by dispersion of silver nanoparticles in polymer along with hexamethylene diisocyanate (HDI) and poly(butadiene adipate).³⁴ Ag-poly(lactic acid) was produced by dispersing carboxylated silver (prepared by thiolation with 3-mercaptopropionic acid) in a solution of poly(lactic acid).³⁵

Applications of Silver-Polymer Nanocomposites

Optical Applications

The optical activity is because of the surface plasmon resonance exhibited by the nanoparticles.

Ag nanoparticles of smaller size in Ag-poly(N-vinylpyrrolidone) (Ag-PVP) showed surface plasmon resonance absorption maximum at 410 nm and also a feature at 350 nm signifying its quantum effects and hence can be used as color filters and /or UV absorbers.³⁶ Ag-poly(vinyl alcohol) (Ag-PVA) plasmonic optical sensor is used for monitoring chicken meat spoilage at room temperature by the color change of the Ag-PVA label from yellow to colorless.³⁷

Electrical Applications

Ag nanoparticles in polyaniline resulted in an increase in electrical conductivity and dielectric properties by two orders of magnitude as compared to pure polyaniline matrix and is used in microelectronic devices.³⁸ Nanocomposites of silver nanowires with polyamide 11 has good electrically conductive applications and hence used for protection of sensitive electrical systems in transportation, automotive industries.³⁹

Antimicrobial Applications

Silver has antimicrobial properties and therefore it inhibits the growth of bacteria. A polymer with its characteristic morphology, serves as a matrix for silver, to be used as an antimicrobial agent. It is accordingly used in various applications. Silver with poly(ethylene

glycol)-poly(urethane-TiO₂) demonstrated excellent activity against *E. coli* and *Bacillus subtilis*.⁴⁰

Ag-poly(vinyl alcohol)-poly(methyl methacrylate) nanocomposites synthesized using radical mediated dispersion polymerization was used as a semitransparent antimicrobial coating.⁴¹ Preservation testing on the Ag-poly(ethylene glycol dimethacrylate) [Ag-poly(EGDMA)] microspheres had shown powerful antimicrobial properties over various bacterial strains and could be used as a preservative.⁴² Ag-chitosan was used in packaging films to protect against moisture, oxygen, flavor, aroma and oil thereby improving the quality of the food products.⁴² Ag nanoparticles with polyurethane was used as an efficient water filter to reduce the risk of water-related diseases like diarrhea and dehydration. Moreover, this nanocomposite was found to be stable and could not be washed by water flow because of the nanoparticles interaction with the nitrogen atom of polyurethane.⁴³ The anti-microbial and anti-fungal activity of the Ag-chitosan-poly(vinyl alcohol) nanocomposites films had demonstrated significant effects against *Escherichia coli* (*E. coli*), *Pseudomonas*, *Staphylococcus*, *Micrococcus*, *Candida albicans* and *Pseudomonas aeruginosa*.²³ To enhance their remedial vigor as anti-microbial agents, curcumin encapsulated chitosan-PVA silver nanocomposites films were developed which showed enormous growth inhibition of *E. coli*.²³ The antibacterial activities of the silver-poly(lactic acid) nanocomposite (Ag-PLA-NC) films were studied against gram-negative bacteria (*Escherichia coli* and *Vibrio parahaemolyticus*) and gram-positive bacteria (*Staphylococcus aureus*) and it was noticed that Ag-PLA-NC films possessed a strong antibacterial activity with an increase in the percentage of AgNPs in the PLA. Thus, Ag-PLA-NC films could be used as an antibacterial scaffold for tissue engineering and medical application.⁴⁴ Silver-silica nanocomposite material

exhibited a very good antimicrobial activity against a wide range of microorganisms because of the release of Ag^+ ions in a more controlled manner and at a lower rate.⁴⁵

Modification of Silver Surface by Thiolation

SAMs are organic assemblies formed by the adsorption of molecular constituents from solution or the gas phase onto the surface of solids or in regular arrays on the surface of liquids (in the case of mercury and probably other liquid metals and alloys). The adsorbates organize spontaneously and sometimes epitaxially into crystalline or semicrystalline structures. There are innumerable head groups that bind to specific metals, alkanethiols ($\text{HS}(\text{CH}_2)_n\text{X}$), dialkyl disulfides ($\text{X}(\text{CH}_2)_m\text{S}-\text{S}(\text{CH}_2)_n\text{X}$), and dialkyl sulfides ($\text{X}(\text{CH}_2)_m\text{S}(\text{CH}_2)_n\text{X}$), where n and m are the number of methylene units and X represents the end group of the alkyl chain ($-\text{CH}_3$, $-\text{OH}$, $-\text{COOH}$). The most widely used head group is acquired from the adsorption of alkanethiols on silver. The thiols largely used are mercaptodecanoic acid, mercaptoethanol, mercaptoethanesulfonic acid and alkyl thiols C_6 - C_{18} which will make them well dispersible in aqueous and organic media.⁴⁶ The tendency to agglomerate was reduced due to the increase in carbon atoms on the silver surface. These long chain alkyl thiols are stable because long chain alkyl thiols are highly ordered on the AgNPs providing an excellent protection of the metal surface against oxidation. They also protect the metal surface by removing the contaminating layers from the surface (Fig. 7).⁴⁶

The alkyl chains are also perpendicular to the silver surface in a self-assembled monolayer of alkane thiolates.⁴⁷ The molecules in a SAM take conformations, that allow intense van der Waals interactions, to minimize the free energy of the organic layer and also to form hydrogen bonds with the neighboring molecules. The binding of an alkanethiol to the surface of the silver

changes the local refractive index and also cause a shift in the surface plasmon frequency. As the length of the alkyl chain increases so is the shift (~ 3 nm to the red for every additional carbon).⁴⁶

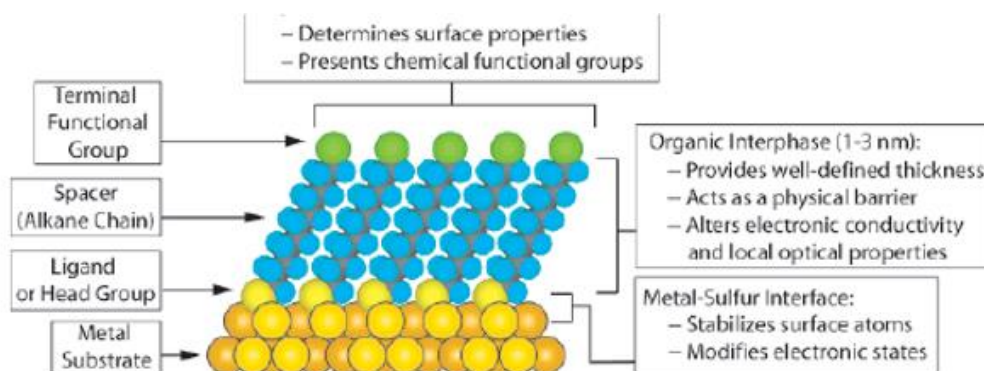


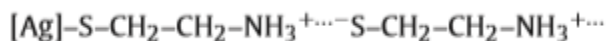
Figure 7: Self-assembled monolayer⁴⁶

The chemical interaction of silver on treatment with organothiols is⁴⁸



The Ag-S bond is a strong covalent bond and this interaction retains the chains on the surface in a long lasting fashion.

Manz et al. reported that the adsorption of benzeneethanethiol, 3-mercaptopropanoic acid, and 3-mercaptopropan-1-ol formed a monolayer on the surface of silver nanoparticles whereas a multilayer was formed due to the significant adsorption of 2-aminoethanethiol on the silver surface. This was due to the formation of ionic bonds by amine groups of adsorbed molecules with slightly acidic thiol groups of the molecules in solution thereby increasing the amount of adsorbed thiol.



It was observed that amino-modified silver exhibited less agglomeration when compared with bare nanosilver. This confirmed that coating of AgNPs created a steric barrier on the surface preventing agglomeration and also increasing the stability of dispersions in organic media. It was

also observed that the presence of the dipole moment in the amino-modified samples favored their solvation by polar solvents like DMF and also adsorption of polymer molecules through their polar functional groups.⁴⁹

Objective

The objective of this work was the development of an effective method for the preparation of silver-polymer nanocomposites containing finely dispersed silver nanoparticles and to utilize these nanocomposites as X-ray contrast and bactericidal agents for biomedical applications.

CHAPTER 2
EXPERIMENTAL METHODS

Chemicals and Reagents

The chemicals used for the synthesis are listed in Table 1.

Table 1: Chemicals

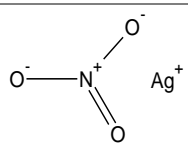

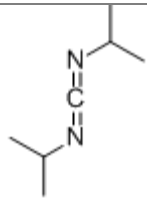
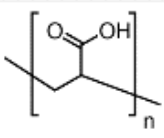
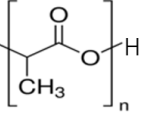
Name	Structure	Characteristics	Manufacturer
Silver nitrate		purity $\geq 99.0\%$ MW=169.87 g/mol mp = 212 °C	Sigma-Aldrich, St. Louis, MO
2-Aminoethane- thiol		purity > 95.0% MW=77.15 g/mol mp = 94 - 99 °C	TCI America, Portland, OR
Silver nanoparticles		particle size = 20-100 nm	Ferro corporation, South Plainfield, NJ
Diisopropyl- carbodiimide		purity $\geq 98.0\%$ MW=126.20 g/mol bp = 145-148 °C	Sigma-Aldrich, St. Louis, MO
Polyacrylic acid		MW = 1800 T _g = 106 °C	Sigma-Aldrich, St. Louis, MO
Poly(D,L- lactide) acid terminated		MW=75,000- 120,000 T _g = 32.9 °C	Sigma-Aldrich, St. Louis, MO

Table 1 (continued)

Poly(D,L-lactide-co-glycolide) ester terminated		lactide: glycolide 85:15 MW=50,000-75,000 T _g = 45-50 °C	Sigma-Aldrich, St. Louis, MO
Poly(D,L-lactide-co-glycolide) acid terminated		lactide: glycolide 50:50 MW=12,000-15,000 T _g = 42-46 °C	Lakeshore Biomaterials, Birmingham, AL
Difco LB agar medium			Becton, Dickinson and Company, Sparks, MD
Hydrochloric acid in methanol		3 M solution	Sigma-Aldrich, St. Louis, MO

The culture used for microbiological study is Escherichia coli strain Dh5a.

Other solvents and reagents used are tetrahydrofuran, N, N-dimethylformamide, acetone, concentrated HNO₃, d-CHCl₃, acetonitrile, NaOH.

Synthetic Procedures

Thiolation of Silver Surface

Ultra-fine, high purity silver powder with the particle size in the range of 20 -100 nm was used for thiolation (Fig. 8). Preceding thiolation, silver was thoroughly washed with deionized water to remove any traces of surfactants. The grafting on the silver surface was accomplished

by adding 10 g sample of nanosilver to 15 mL of THF containing 2×10^{-3} mmol of 2-aminoethanethiol. This suspension was stirred for 1 h, filtered, washed with THF and then air-dried overnight.

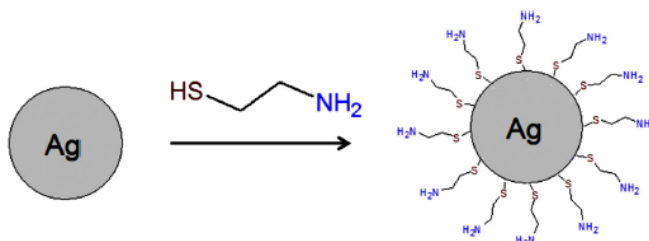


Figure 8: Thiolation of silver surface

Synthesis of Silver-Polymer Nanocomposites

The silver-polyacrylic acid (Ag-PAA) material was obtained by condensation of carboxyl groups of PAA with amino groups of the grafted 2-aminoethanethiol.

PAA (2 g) was dissolved in 20 mL DMF on a hot plate. Amino-modified AgNPs weighing 0.002 g, 0.01 g, 0.02 g, 0.04 g and 0.1 g were then dispersed in 20 mL of 10% solution of PAA in DMF using an Ultra-Turrax T25 disperser (IKA Works, Inc., Wilmington, NC). This was followed by dropwise addition of 0.05 g of crosslinker, diisopropylcarbodiimide (DIPC), dissolved in 1 mL DMF, to the amino-modified AgNPs, which had been dispersed in PAA. These solutions were stirred for 3 h at room temperature. They were then transferred to a rotary evaporator for the evaporation of DMF. The residue was then washed with acetone and air-dried overnight to form Ag-PAA material.

Silver-poly(methylacrylate) (Ag-PMA) (**1**) nanocomposites were prepared by acid-catalyzed esterification of the remaining COOH groups of grafted PAA. The obtained Ag-PAA samples (1 g) were weighed and dispersed in 50 mL hydrochloric acid in methanol. This reaction mixture was refluxed for 30 min. The solvent was then evaporated on an ultrasonic base for even

dispersion of nanoparticles. The residue attained was dried under vacuum at 110 °C for 2 h (Fig. 9).

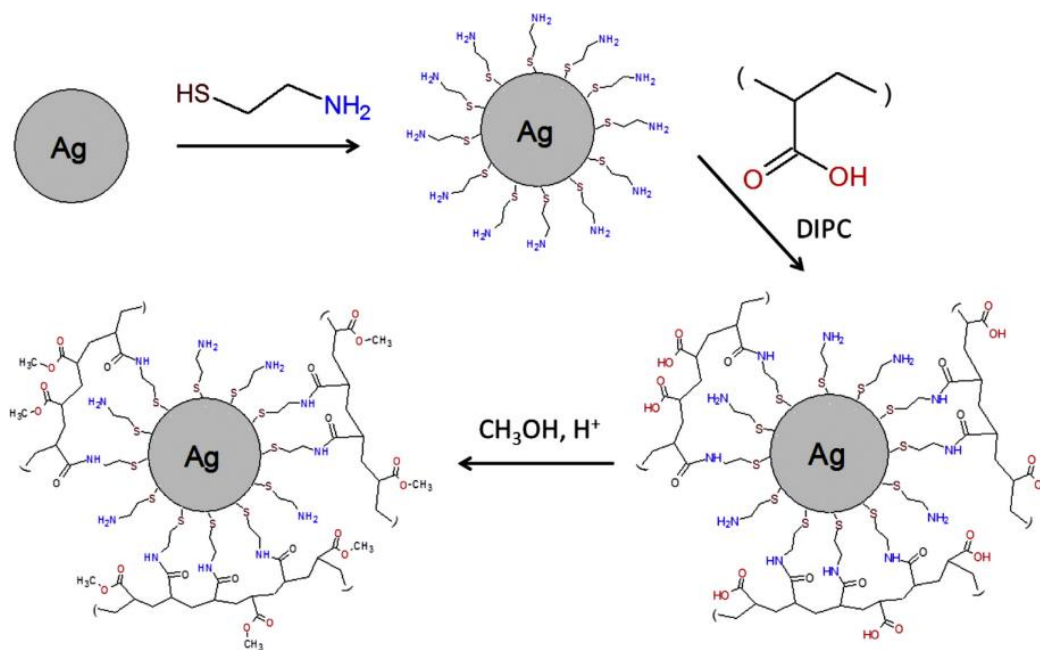


Figure 9: Synthesis of Ag-PMA (1)

Acid terminated PLA (2 g) was dissolved in 40 mL DMF, ester terminated PLGA (3 g) was dissolved in 60 mL DMF, an acid terminated PLGA (3 g) was dissolved in 60 mL DMF and DIPC (0.5 g) was dissolved in 10 mL of DMF respectively. This was subsequently superseded by the dispersion of different amounts of 0.02 g, 0.03 g, and 0.03 g of amino-modified AgNPs in 20 mL of PLA solution, 30 mL of PLGA (ester terminated) solution and 30 mL of PLGA (acid terminated) solution. DIPC solution (0.1 mL) was added dropwise to each dispersion of amino-modified AgNPs. The dispersion was then sonicated for 10 min on a Fisher Scientific ultrasonic bath. The sonication was repeated once again for 10 min with the remaining 20 mL of PLA solution, 30 mL of PLGA (ester terminated) solution and 30 mL of PLGA (acid terminated) solution for even dispersion of Ag nanoparticles. The non-dispersed silver was separated and the solvent was evaporated in the rotary evaporator for 2.5 h. The obtained product silver-poly(DL-

lactide), the acid terminated Ag-PLA (**2**); silver-poly(DL-lactide-co-glycolide), ester terminated Ag-PLGA (**3**), and silver-poly(DL-lactide-co-glycolide), acid terminated Ag-PLGA (**4**) were washed with ethanol and then dried under vacuum overnight (Fig. 10).

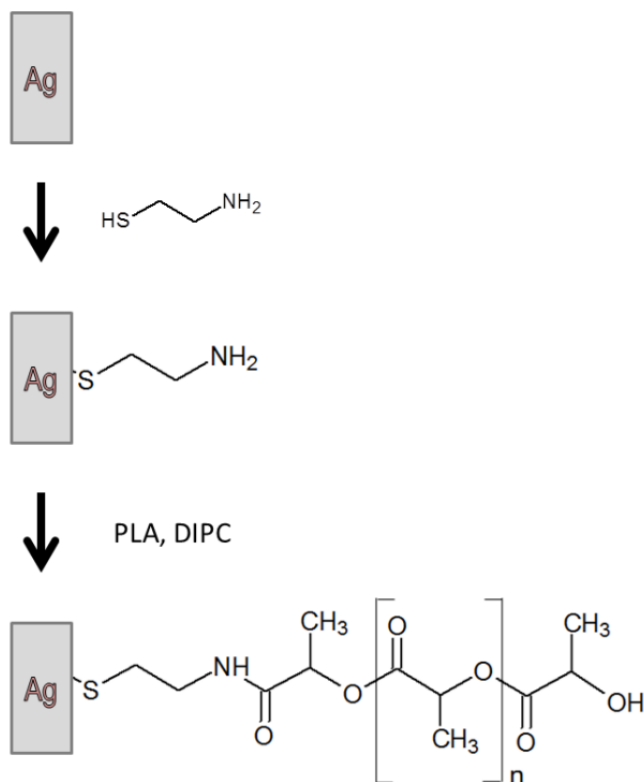


Figure 10: Scheme of the synthesis of nanocomposites **2-4**

Characterization

Atomic Absorption Spectroscopy

The contents of silver in the samples were determined by a Shimadzu AA 6300 atomic absorption spectrometer at $\lambda = 328$ nm. Ag-PAA samples (0.043 g) were dissolved in concentrated HNO₃ and diluted to 50 mL with distilled water.

The samples **2-4** (0.08 g) were dissolved in 5 mL concentrated HNO₃ by slight warming. The solution was then diluted to 20 mL with distilled water and filtered. The filtrate was collected separately in a beaker. The residue was washed well with distilled water and then

washed with 5 mL concentrated 20% NaOH. This filtrate was added drop by drop to the filtrate that was collected initially in a beaker (prepared with concentrated HNO₃) and then tested with the pH paper until it turned neutral. The residue on the filter paper was added to the filtrate and was dissolved by heating. The solution that was obtained was diluted to 50 mL with distilled water.

Determination of Polymer Contents by Weight Method

The amount of polymers bonded to silver were calculated using weight method. The nanocomposites **2-4** (0.5 g), containing known amount of silver, were weighed and dispersed in 15 mL of acetonitrile. The insoluble silver was separated using a Sorvall Legend XI centrifuge (Thermo Fischer Scientific, Waltham, MA) for 15 min at 14,000 rpm. The solution was removed from the precipitate and the procedure was repeated with pure acetonitrile twice. The precipitate that was obtained was dried under vacuum overnight and the weight of the coated silver was determined on analytical balances.

NMR Spectroscopy

NMR spectra of Ag-PMA (**1**) sample were obtained using d-CHCl₃ in a JEOL Oxford AS400 spectrometer at 399.8 (¹H) and 100.5 (¹³C) MHz.

X-ray Diffraction Analysis

X-ray diffraction analysis of Ag-PMA (**1**) was conducted on a DRON 2.0 X-ray diffractometer. The monochromatic Cu-K α radiation filtered by Ni, with $\lambda = 0.154$ nm was provided by an IRIS-M7 generator at 30 kV and a current of 30 mA. The scattering intensities were measured by a scintillation detector at 0.2° steps in the range of $2\theta = 3-60^\circ$.

Transmission Electron Microscopy

TEM image of Ag-PMA (**1**) was obtained with a Topcon EM 200 electron microscope at 80 kV. The sample was dispersed in a 50% ethanol solution using a W-385 sonicator for 2 min before imaging.

Fourier Transform Infrared Spectroscopy

FT-IR spectra of the Ag-PMA (**1**) samples were recorded on a Shimadzu Prestige-21 FT-IR spectrometer (Kyoto, Japan). The preparation of samples **2-4** for FTIR was similar to the method described in 2.3.2. A small amount of well-powdered samples **2-4** were placed on the sample holder and FT-IR spectra were recorded.

Ultraviolet-Visible Spectroscopy

UV-vis spectra of surface plasmon resonance of samples **2-4** were recorded on a Shimadzu UV-1700 PharmaSpec instrument (Kioto, Japan). The samples were dispersed in DMF on a Fisher Scientific ultrasonic bath for 10 min before the measurements were taken. The solutions of corresponding polymers were used as reference solutions.

Scanning Electron Microscopy

SEM images of samples **2-4** were obtained utilizing a Zeiss DSM 940 scanning electron microscope (Jena, Germany) at 20 kV. The samples were deposited on a copper support without sputter coating and then loaded onto the SEM holder.

X-ray Imaging

X-ray images of samples **2-4** were obtained using a Philips Bucky Diagnost apparatus (Amsterdam, Netherlands) at 40 kV and 0.8 mA. The exposure time was 4 ms. The samples for imaging were prepared by placing the materials between two glass slides and the thickness of the samples was 1mm.

Microbiological Study

The solutions for the toxicological study of samples **2-4** were prepared by dissolving these materials (5 wt%) in acetonitrile. The solutions were well sonicated in an ultrasonic bath to achieve the fine dispersion of AgNPs. Solutions of corresponding polymers of the same concentration were used as control solutions. A 20 μL portion of each sample solution was transferred on an agar medium in a petri dish. After drying the samples, *E. coli* was cultured on the media at 37 °C for 24 h.

CHAPTER 3

RESULTS AND DISCUSSION

Ag-PAA Nanocomposites

Composition

Ag-PAA samples were prepared by the reaction of five different amounts of amino-modified silver nanoparticles with polyacrylic acid. Atomic absorption spectroscopy (AAS) was used to determine the Ag content in the five Ag-PAA samples and it appeared that these samples consisted 0.2, 0.5, 0.9, 1.4 and 2.7 wt% of silver. The samples were dark gray and contained fully agglomerated Ag nanoparticles (Fig. 11).

Esterification reaction was performed on these samples and the samples with 0.2-0.9 wt% of silver rapidly became clear demonstrating its total dissolution and formation of fine colloidal dispersions of Ag nanoparticles. It was perceived that the sample with 1.4 wt% of silver displayed some cloudiness in the solution, nonetheless the solution was stable without any precipitation. The evaporation of the solvent resulted in a light yellowish transparent composite material. The sample with 2.7 wt% of silver was not dispersed wholly and the precipitation of silver was noticed (Fig. 11)

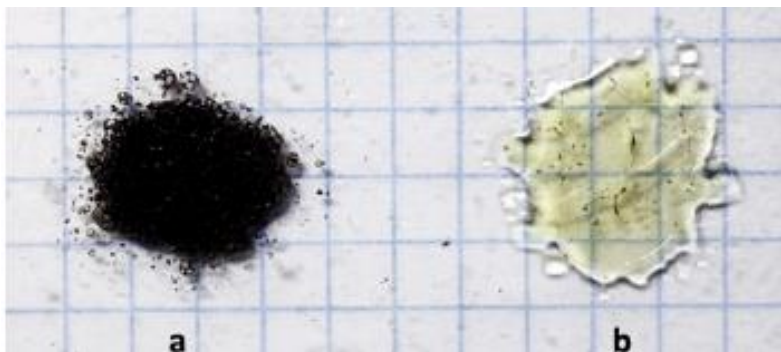


Figure 11: Agglomeration and deagglomeration of silver nanoparticles (a: Ag-PAA, b: Ag-PMA)

Fourier Transform Infrared Spectroscopy

The esterification of carboxyl groups was confirmed by FT-IR spectroscopy. The $\nu_{(C=O)}$ band observed at 1703 cm^{-1} in the IR spectrum of PAA (Fig. 12)⁵⁰ was shifted to 1720 cm^{-1} in the Ag-PMA (**1**) sample. The broad band of COOH groups at $3500\text{-}2500\text{ cm}^{-1}$ was moved to 3372 cm^{-1} depicting a decrease in intensity of the COOH band. This band could be associated with the still existing free COOH groups which have a diminished aptitude to H-bonding. There was an increase in the intensity of $\nu_{(CH)}$ bands which was visible by its shift from 2939 to 2955 cm^{-1} proving the presence of the OCH₃ group.⁵¹ A band at 887 cm^{-1} also confirmed the existence of OCH₃ group (Fig. 13)

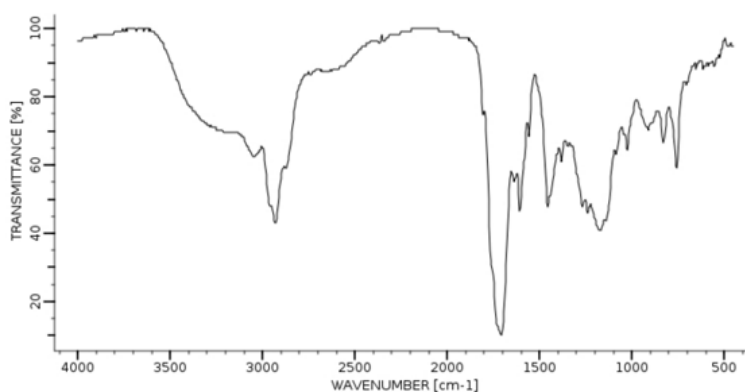


Figure 12: IR spectrum of Polyacrylic acid

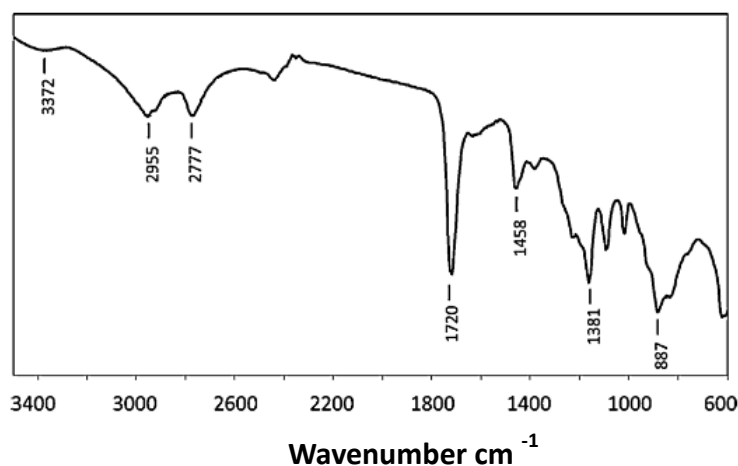


Figure 13: FT-IR spectrum of Ag-PMA

Nuclear Magnetic Resonance Spectroscopy

NMR spectroscopy was used to confirm the esterification of carboxyl groups in the ^1H NMR spectrum of Ag-PMA (**1**). The signals at 1.5-2.2 ppm (bm, CH_2) and 3.4 ppm (s, CH) were similar to the corresponding signals for PAA.⁵² However, an additional signal was observed at 3.6 ppm pertaining to a singlet, CH_3O group. The signal at 8.9 ppm (bs, COOH) could be attributed to the existing isolated carboxyl groups.⁵³ This signal was not present in the spectrum of PAA, as the H-bonding between COOH groups shifted this signal to 12.2 ppm. In the ^{13}C NMR spectrum, the signals at 23, 26 and 28 ppm represented CH_2 group and the signal at 41 ppm was identified as CH group. The signals at 52 ppm and 176 ppm were portrayed as CH_3O and $\text{C}=\text{O}$ groups respectively (Fig. 14).

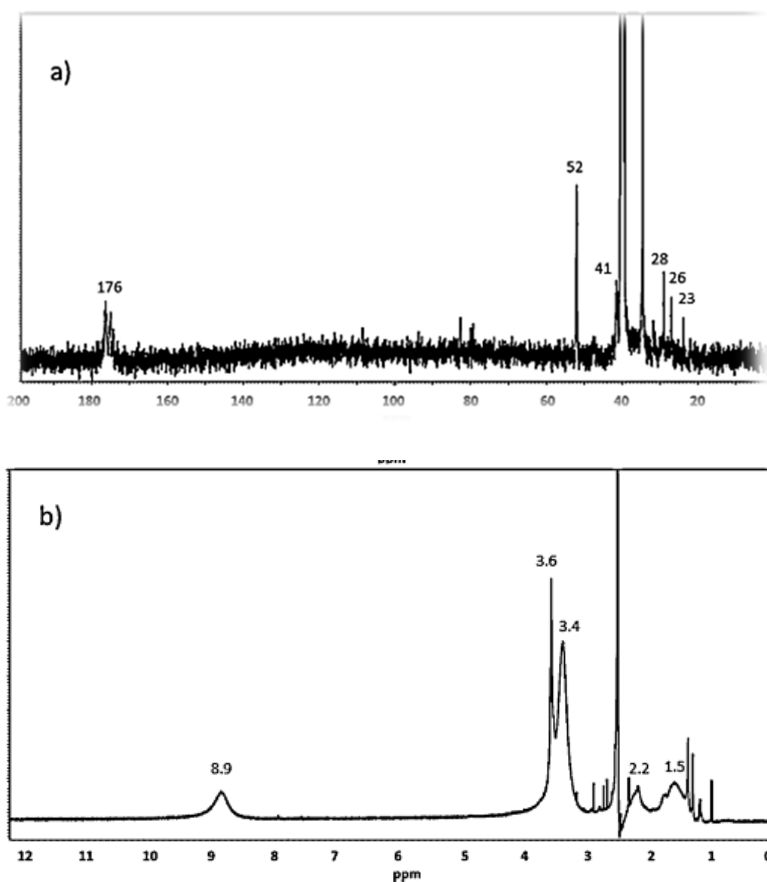


Figure 14: NMR Spectra of Ag-PMA (a: ^{13}C NMR; b: ^1H NMR)

Transmission Electron Microscopy

The presence of silver in Ag-PMA was confirmed by TEM. This imaging showed no agglomeration of the Ag nanoparticles (Fig. 15) and the mean particle diameter calculated using Image J v.1.47 software was 62 nm.

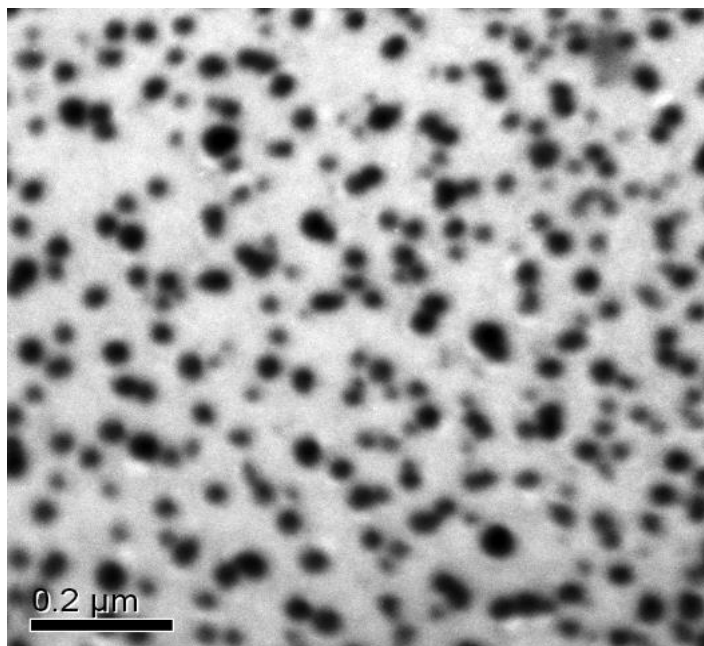


Figure 15: TEM image of Ag-PMA

X-ray Diffraction Spectrometry

X-ray diffraction occurs when X-rays are scattered from the periodic array of atoms within a crystal. The positions of the diffraction peaks are associated to the distance between parallel planes of atoms and the intensity of the peaks are determined by the arrangement of the atoms in the crystal. These planes of atoms produce a diffraction peak at a specific angle 2θ .⁵⁴ It was observed that Ag [111] and Ag [200] attained characteristic diffraction peaks at $2\theta = 38.2^\circ$ and 44.4° , respectively. The peak at the detector angle $2\theta = 44.4^\circ$ was found to be very weak. The broadening of X-ray diffraction line, determines the particle size, for crystallites smaller than 1000 \AA diameter. This broadening was observed at Ag [111] and can be attributed to the

small size of the nanoparticles. The crystallite size was estimated from the Ag [111] peak width at half maximum using Debye-Scherrer formula and was found to be 27 nm. Debye-Scherrer formula is

$$D = K\lambda / B \cos \Theta$$

where D is the diameter of the particle, K = 0.89 (constant), B is the broadening of the line, λ is the wave-length of the X-ray radiation, and Θ is the Bragg angle. B must be corrected for the width of the diffraction line for large particles, known as the instrument width. The correction appears as

$$B = B' - b'$$

where B is once again the broadening, B' is the width of the line from the small particles, and b' is the instrument width or the width of the line from particles larger than 1000 Å⁵⁵ (Fig. 16).

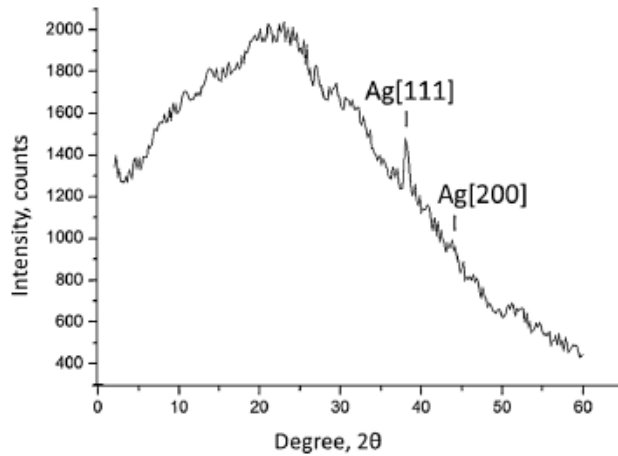


Figure 16: XRD Spectrum of Ag-PMA

Ag-PLA and Ag-PLGA Nanocomposites

Composition

The content of dispersed silver in Ag-PLA (2), Ag-PLGA (3), Ag-PLGA (4) nanocomposites were determined using atomic absorption spectrometry. The largest amount of

nanosilver was found to be dispersed in PLA. Ester-terminated PLGA showed lower ability to disperse nanosilver as compared to acid terminated PLGA. Nevertheless, the amount of surface bonded polymer in ester terminated PLGA determined by weight method was found to be maximum (Table 2).

Table 2: Contents of Silver in Materials

Material	Contents of pure Ag (wt%)	Contents of coated Ag (Ag + polymer) (wt%)
Ag-PLA	0.12	0.38
Ag-PLGA (ester terminated)	0.05	0.88
Ag-PLGA (acid terminated)	0.09	0.47

FT-IR Spectra

FT-IR spectrum did not display any notable bands in case of bare nanosilver. Material **2** exhibited distinctive bands in agreement with polylactic acid. A band at 1739 cm^{-1} revealed the presence of a carbonyl group. The bands at $2839\text{-}2947$ and 1453 cm^{-1} could be connected to stretching and bending vibrations of CH_3 groups. Deformational and asymmetric vibrations of C-H bond was accounted for the band at 1372 cm^{-1} . The weak band at 1215 cm^{-1} was correlated to C-O-C stretching vibrations in polyesters. A band at 1102 cm^{-1} was associated with C-O-C asymmetric vibrations.⁵⁶ A broad band visible at 1592 cm^{-1} was identified with carboxylate ions. The spectra of materials **3** and **4** were almost identical to the spectrum of sample **2** except for the weak bands of CH_3 groups. Overall, the bands in the fingerprint region (1500 cm^{-1}) were very intense and broad (Fig. 17).

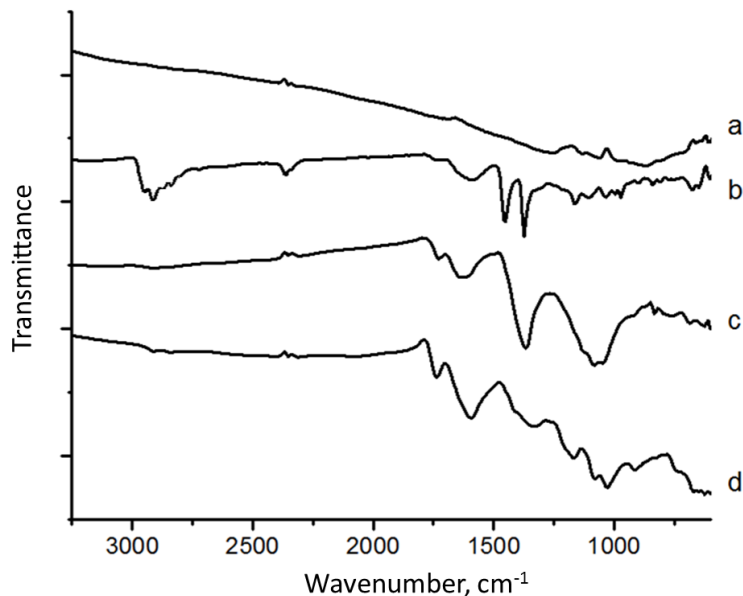


Figure 17: FT-IR spectra (a: AgNPs, b: Ag-PLA (2), c: Ag-PLGA (3), d: Ag-PLGA (4))

UV-Vis Spectra

The spectra of dispersion of materials **2-4** displayed broad bands at 454-479 nm. However, the dispersion of bare nanosilver in DMF did not exhibit any surface plasmon resonance absorption band (Fig. 18).

SEM

The images obtained by SEM confirmed high dispersibility of silver nanoparticles in PLA. The average particle size of material **2** presented 100 nm without any agglomerates. Even though the silver nanoparticles in material **3** were densely agglomerated with the average particle size to be 1-2 μm , few isolated nanoparticles were visible in this material. Material **4** had some small agglomerates, nonetheless, a great amount of nanosilver emerged as isolated nanoparticles and their average particle size was observed as 200 nm (Fig. 19).

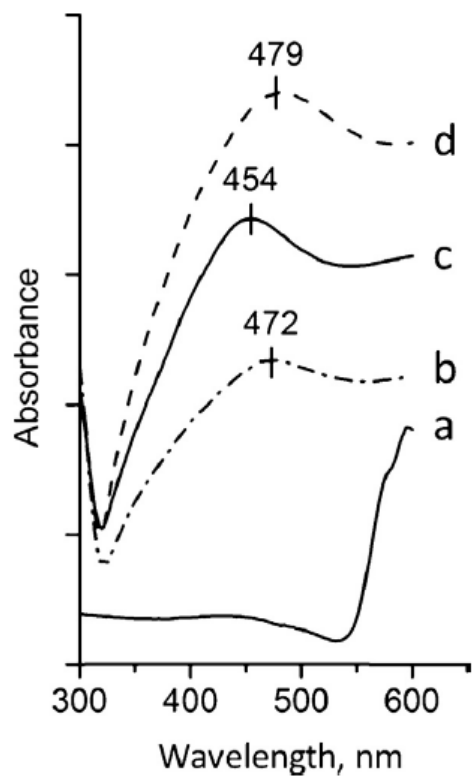


Figure 18: UV-vis spectra (a: AgNPs, b: Ag-PLA (2), c: Ag-PLGA (3), d: Ag-PLGA (4))

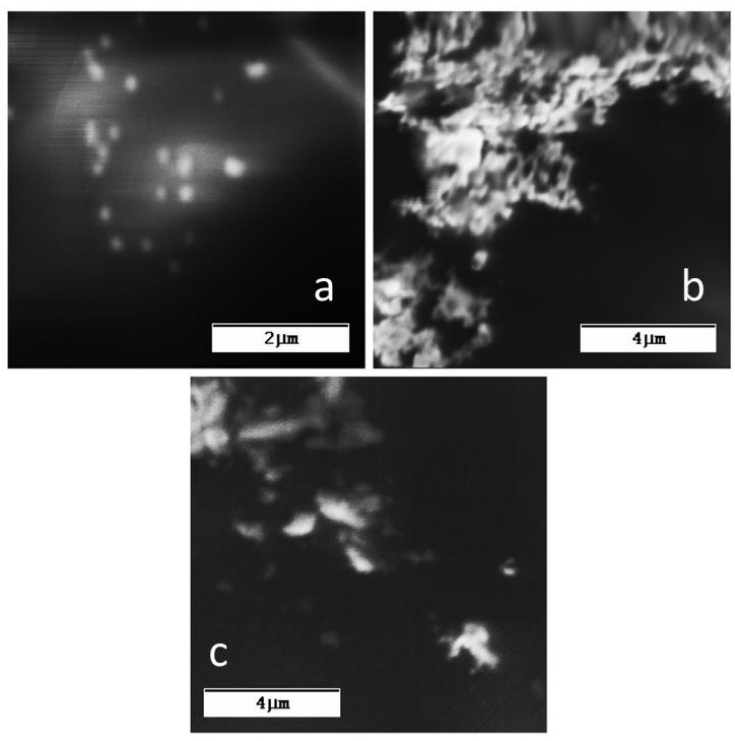


Figure 19: SEM images (a: Ag-PLA (2), b: Ag-PLGA (3), c: Ag-PLGA (4))

X-ray Images

X-ray images of the materials **2-4** are shown in Fig. 20. Despite the contents of silver being low, X-rays were absorbed by silver and its absorption was clearly visible on the image.

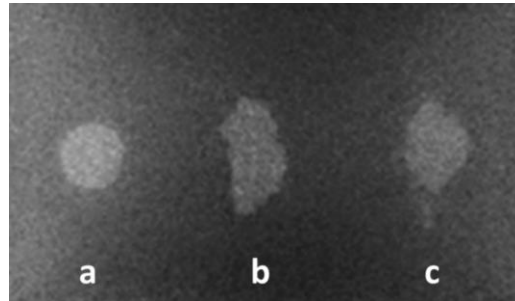


Figure 20: X-ray images (a: Ag-PLA (**2**), b: Ag-PLGA (**3**), c: Ag-PLGA (**4**))

Toxicological Effect against E. coli.

The inhibiting effect of the polymers was not detected in the control experiment, however, the inhibiting effect of nanosilver against *E. coli* was distinctly visible after incubating the media. The sizes of the inhibitory zones were 4-8 mm for samples **2** and **4** and 6-12 mm for sample **3** (Fig. 21).

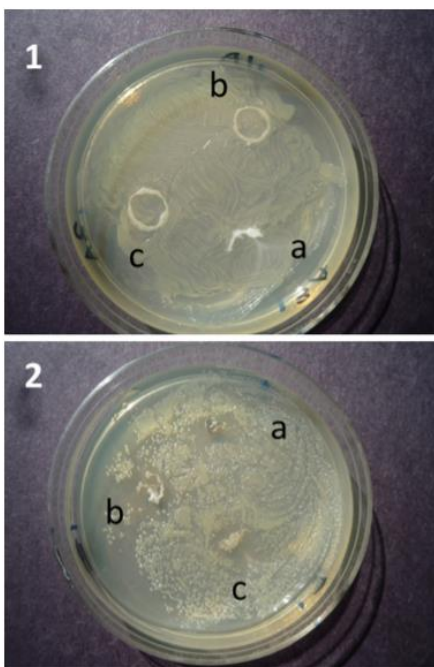


Figure 21: Antibacterial activity of pure polymers (1): (a: PLA, b: PLGA (ester terminated), c: PLGA (acid terminated)) and silver-polymer materials (2): (a: Ag-PLA (**2**), b: Ag-PLGA (**3**), c: Ag-PLGA (**4**))

Discussion

Ag-PAA Nanocomposites

The development of self-assembled monolayers with end functional groups, on the surface of silver, using thiolation, is quite popular. Hydrophobization of the silver surface employing 2-aminoethanethiol enhances the dispersibility of silver nanoparticles considerably. But, it is perceived that the amination of AgNPs could not restrain its agglomeration fully, necessitating more modification.⁴⁹

The modification was done using polyacrylic acid, which was covalently bonded to the silver nanoparticles, by condensation of carboxyl groups with the surface amino groups using the carbodiimide method. Considering the solubility of its by-product, diisopropylurea in almost all organic solvents, DIPC was selected as a coupling reagent.

The product acquired in the condensation reaction contained highly agglomerated AgNPs. This immense agglomeration of nanoparticles in Ag-PAA was a result of a large number of free carboxylic acid groups that could participate in intermolecular hydrogen bonding interactions with like molecules functioning both as a H-bond donor and acceptor. It was also reported that polyacrylic acid favored agglomeration of nanosilver, synthesized by the reduction method.⁵⁷ The free carboxylic acid groups of PAA were subjected to acid-catalyzed esterification with methanol in the presence of HCl as a catalyst for the elimination of hydrogen bonding interactions. The disappearance of intermolecular H-bonds between carboxylic groups of PAA, which were responsible for agglomeration,⁵⁸ in the esterification reaction, resulted in the deagglomeration of amino-modified AgNPs as well as significant softening of the composite.

The average particle size of AgNPs estimated from X-ray diffraction data was lower than TEM data because larger size particles did not contribute to the broadening of the peak. In any case, both the methods proved that the nanoparticles were not agglomerated.

It had been recorded that stable colloidal solutions of AgNPs were obtained only at low contents of silver (up to 0.1 wt %) ⁵⁹. Silver-polymer nanocomposites with the average particle size below 20 nm were found to be less stable due to the low-temperature sintering of silver nanoparticles. ^{60, 61} The average particle size of 27 nm obtained by XRD analysis, and the average particle size of 62 nm attained by TEM, confirmed that the uniform embedding of AgNPs onto the polymer matrix could be accomplished at a relatively large size of the particles (up to 100 nm).

Ag-PLA and Ag-PLGA Nanocomposites

Carbodiimide chemistry proved high efficacy in coating silver nanoparticles with PLA, ester terminated PLGA and acid terminated PLGA. Carbodiimides were utilized as stabilizing agents, coupling agents and as condensation agents during the reaction. Different types of substituted carbodiimides form amide bond in the reaction between COOH and NH₂ groups. ⁶² DIPC was preferred among numerous carbodiimides, not only due to the enhanced solubility of its by-product, diisopropylurea in many organic solvents but also its easy removal from the material by repeated washings.

The reaction of amines with acid-terminated polymers PLA and PLGA took place. It was assumed that the reaction of ester terminated polymer PLGA with the amines would not occur. But it was found that the product (**3**) also contained polymer-coated silver nanoparticles despite the low content of silver in the polymer matrix. This unusual reaction was due to the aminolysis of the ester bond in the polymer chain by the surface amino groups (Fig. 22) producing OH and

surface CONH groups. Similarly, Croll et al. had performed surface modification of PLGA by aminolysis under mild conditions using polar aprotic solvents.⁶³

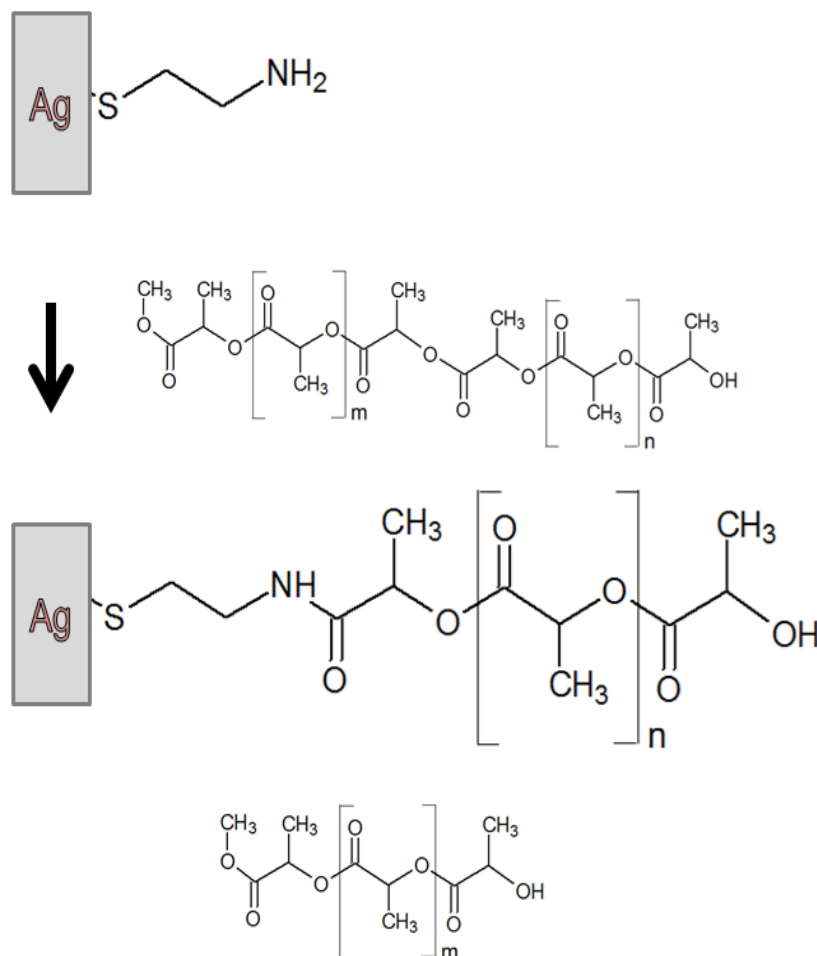


Figure 22: Surface aminolysis of Ag-PLGA (3)

Chemisorption of a large amount of ester terminated PLGA on Ag nanoparticles could be interpreted to the smaller size of AgNPs in Ag-PLGA (3) in contrast with Ag-PLA (2) and Ag-PLGA (4). The dispersibility of nanosilver in PLGA (ester terminated) was very low proving the dispersal of only small sized AgNPs. However, large AgNPs got precipitated from the reaction mixture. Acid terminated polymers had higher stabilizing ability than ester terminated polymers due to a large range of sizes of nanoparticles.

FT-IR spectra of polymer coated AgNPs included primarily the same characteristic bands of the corresponding polymers confirming the coating of AgNPs with the polymers.

The surface plasmon resonance, absorption maximum of amino-modified silver nanoparticles dispersed in DMF was found to be 470 nm.⁴⁹ The samples Ag-PLA (2) and Ag-PLGA (4) had their absorption maxima band shifted to 472 and 479 nm (longer wavelengths) whereas Ag-PLGA (3) had its absorption maximum at 454 nm (shorter wavelength). Since the SPR absorption maximum changed due to the size of the particle, it was inferred that this shift to shorter wavelength had been caused by the small size of AgNPs in sample 3.⁶⁴ The content of silver in this sample was nearly twice lower than those of Ag in samples 2 and 4. The small size of the Ag nanoparticles in ester-terminated Ag-PLGA (3), resulted in the significant reduction in its dispersibility as compared to the acid-terminated polymers. Moreover, it was observed that almost all the large nanoparticles in Ag-PLGA (3) were precipitated. Huang et al. had indicated that SPR absorption maximum depended on the size of the particle and increase in particle size resulted in the shift to longer wavelengths⁶⁵ which was observed in acid terminated Ag-PLA (2) and Ag-PLGA (4). This outcome was in accordance with the chemical composition data. The spectra also displayed the absorbance of bare Ag nanoparticles to be greater than 550 nm, which was indicative of complete agglomerated silver.

Agglomerated AgNPs along with few isolated nanoparticles were observed in the SEM image of ester-terminated Ag-PLGA (3), indicating the small size of the nanoparticles and its low dispersibility. However, the acid terminated polymers Ag-PLA (2) had no agglomerates and Ag-PLGA (4) had isolated nanoparticles signifying greater dispersibility due to the large size of the nanoparticles.

X-ray imaging showed almost similar absorption of X-rays in samples **2-4**. This was due to the higher atomic number of Ag ($Z = 47$) and the K-edge of silver (25.5).⁶⁵ This K-edge is the ideal binding energy for the absorption of the X-ray beam. Ag being an anti-microbial agent has greater advantages and could be used as X-ray visible biomaterials in the field of medicine (for example, orthopedic or cardiovascular applications).

The obtained nanocomposites showed inhibition in the growth of bacteria. Ag-PLGA (**3**) with low silver content had stronger bactericidal effect in comparison with samples **2** and **4**. This inhibition effect was on account of the small size of the AgNPs and / or the release of Ag^+ ions from the surface. The particle size plays an important role in the inhibition of bacteria.^{67, 68, 69} This was evident from UV-vis study which confirmed that material **3** contained predominantly smaller Ag nanoparticles in contrast to samples **2** and **4** and that could be one of the reasons of the difference in bio-toxicity of these materials.

Conclusions

1. The surface of nanosilver was successfully modified by 2-aminoethanethiol.
2. Amino-modified nanosilver was covalently bonded to polyacrylic acid, biodegradable polymers like acid terminated polylactic acid, ester terminated poly(D,L-lactide-co-glycolide) and acid terminated poly(D,L-lactide-co-glycolide) in the presence of diisopropylcarbodiimide by carbodiimide method.
3. Esterification of Ag-PAA by hydrochloric acid in methanol resulted in deagglomeration of agglomerated AgNPs, thereby producing Ag-poly(methylacrylate) (Ag-PMA) with finely dispersed nanosilver.
4. Ag-PMA samples containing silver up to 1.4 wt% showed good dispersibility. The materials obtained were transparent and light yellowish in color.

5. The average particle size of 27 nm obtained by XRD analysis, and the average particle size of 62 nm attained by TEM, confirmed that the uniform embedding of AgNPs onto the polymer matrix could be accomplished at a relatively large size of the particles (up to 100 nm).
6. Poly(D,L-lactide-co-glycolide), ester terminated reacted with amino-modified nanosilver by aminolysis of the ester bond.
7. Silver-polymer nanocomposites obtained using acid-terminated polymers PLA and PLGA contained highly dispersed nanosilver in polymer matrix whereas dispersibility of AgNPs in ester-terminated PLGA was very low.
8. Absorption of X-rays by samples **2-4** demonstrated X-ray contrast properties of silver.
9. The obtained nanocomposites **2-4** showed inhibition in the growth of bacteria, however, material **3** manifested stronger bactericidal effect.

REFERENCES

- [1] Faraday, M. The Bakerian Lecture: Experimental Relations of Gold (and Other Metals) to Light. *Philosophical Transactions of the Royal Society of London* 1857, 147, 145.
- [2] Horry, R.; Jardine B. 'Michael Faraday's microscope slide', Explore Whipple Collections, Whipple Museum of the History of Science, University of Cambridge, 2008
[<http://www.hps.cam.ac.uk/whipple/explore/microscopes/faradaysslide/>, accessed 08 March 2016]
- [3] Filipponi, L.; Southerland, D. Fundamental 'Nano-Effects'. In *NANOTECHNOLOGIES: Principles, Applications, Implications and Hands-on Activities*; Publications Office of the European Union: Luxembourg, 2013; p 63.
- [4] Goesmann, H.; Feldmann, C. Nanoparticulate Functional Materials. *Angewandte Chemie, International Edition* 2010, 49 (8), 1362.
- [5] Eustis, S.; El-Sayed, M. A. Why Gold Nanoparticles Are More Precious than Pretty Gold: Noble Metal Surface Plasmon Resonance and Its Enhancement of the Radiative and Nonradiative Properties of Nanocrystals of Different Shapes. *Chemical Society Reviews* 2006, 35 (3), 209.
- [6] Boysen, E.; Muir, N. C. *Nanotechnology for Dummies*, 2nd ed.; Wiley, John & Sons: The United Kingdom, 2011.
- [7] Schmid, G.; Corain, B. Nanoparticulated Gold: Syntheses, Structures, Electronics, and Reactivities. *ChemInform* 2003, 34 (44), 3081.
- [8] Zhu, Y.; Xu, F.; Qin, Q.; Fung, W. Y.; Lu, W. Mechanical Properties of Vapor–Liquid–Solid Synthesized Silicon Nanowires. *Nano Letters* 2009, 9 (11), 3934.

- [9] Zielińska, A.; Skwarek, E.; Zaleska, A.; Gazda, M.; Hupka, J. Preparation of Silver Nanoparticles with Controlled Particle Size. *Procedia Chemistry* 2009, 1 (2), 1560.
- [10] Rashid, M. U.; Bhuiyan, M. K. H.; Quayum, M. E. Synthesis of Silver Nano Particles (Ag-NPs) and Their Uses for Quantitative Analysis of Vitamin C Tablets. *Journal of Pharmaceutical Sciences* 2013, 12 (1), 29.
- [11] Guzmán, M. G.; Dille, J.; Godet, S. Synthesis of Silver Nanoparticles by Chemical Reduction Method and Their Antibacterial Activity. *International Journal of Chemical and Biomolecular Engineering* 2008, 7 (7), 91.
- [12] Pacioni, N. L.; Borsarelli, C. D.; Rey, V.; Veglia, A. V. Synthetic Routes for the Preparation of Silver Nanoparticles: A Mechanistic Perspective. In *Silver Nanoparticle applications: In the fabrication and design of medical and Biosensing devices*; Udekwu, K. I., Alarcón, E. I, Griffith, M., Eds.; Springer International Publishing AG: Switzerland, 2015; 13.
- [13] Lopatynskyi, A. M.; Lopatynska, O. G.; Guo, L. J.; Chegel, V. I. Localized Surface Plasmon Resonance Biosensor—Part I: Theoretical Study of Sensitivity—Extended Mie Approach. *IEEE Sensors Journal* 2011, 11 (2), 361.
- [14] Plasmonics. nanoComposix <http://nanocomposix.com/pages/plasmonics> (accessed Mar 28, 2016).
- [15] Silver Nanoparticles: Optical Properties. nanoComposix <http://nanocomposix.com/pages/silver-nanoparticles-optical-properties> (accessed Mar 28, 2016).
- [16] Osman, M. A.; Keller, B. A. Wettability of Native Silver Surfaces. *Applied Surface Science* 1996, 99 (3), 261.

- [17] Morones, J. R.; Elechiguerra, J. L.; Camacho, A.; Holt, K.; Kouri, J. B.; Ramírez, J. T.; Yacaman, M. J. The Bactericidal Effect of Silver Nanoparticles. *Nanotechnology* 2005, 16 (10), 2346.
- [18] AshaRani, P. V.; Low Kah Mun, G.; Hande, M. P.; Valiyaveetil, S. Cytotoxicity and Genotoxicity of Silver Nanoparticles in Human Cells. *ACS Nano* 2009, 3 (2), 279.
- [19] Zhang, T.; Wang, L.; Chen, Q.; Chen, C. Cytotoxic Potential of Silver Nanoparticles. *Yonsei Medical Journal* 2014, 55 (2), 283.
- [20] Reidy, B.; Haase, A.; Luch, A.; Dawson, K.; Lynch, I. Mechanisms of Silver Nanoparticle Release, Transformation, and Toxicity: A Critical Review of Current Knowledge and Recommendations for Future Studies and Applications. *Materials* 2013, 6 (6), 2295.
- [21] Zhou, W.; Ma, Y.; Yang, H. A Label-Free Biosensor Based on Silver Nanoparticles Array for Clinical Detection of Serum p53 in Head and Neck Squamous Cell Carcinoma. *International Journal of Nanomedicine* 2011, 11 (6), 381.
- [22] Ozin, G.; Kirkby, S.; Mesaros, M.; Ozkar, S.; Stein, A.; Stucky, G. Intrazeolite Semiconductor Quantum Dots, and Quantum Supralattices: New Materials for Nonlinear Optical Applications. In *Materials for Nonlinear Optics, Chemical Perspectives*; Marder, S., Sohn, J., Stucky, G., Eds.; American Chemical Society: Boston, Massachusetts, 1991; Vol. 4, pp 310–311.
- [23] Li, H.-J.; Zhang, A.-Q.; Hu, Y.; Sui, L.; Qian, D.-J.; Chen, M. Large-Scale Synthesis and Self-Organization of Silver Nanoparticles with Tween 80 as a Reductant and Stabilizer. *Nanoscale Research Letters* 2012, 7 (1), 612.

- [24] Vimala, K.; Yallapu, M. M.; Varaprasad, K.; Reddy, N. N.; Ravindra, S.; Naidu, N. S.; Raju, K. M. Fabrication of Curcumin Encapsulated Chitosan-PVA Silver Nanocomposite Films for Improved Antimicrobial Activity. *Journal of Biomaterials and Nanobiotechnology* 2011, 2 (1), 55.
- [25] Porel, S.; Ramakrishna, D.; Hariprasad, E.; Gupta, D.; Radhakrishnan, P. Polymer Thin Film with in Situ Synthesized Silver Nanoparticles as a Potent Reusable Bactericide. *Current Science* 2011, 101 (7), 927.
- [26] Wankhade, Y.; Kondawar, S.; Thakare, S.; More, P. Synthesis and Characterization of Silver Nanoparticles Embedded in Polyaniline Nanocomposite. *Advanced Materials* 2013, 4 (1), 89.
- [27] Guo, Q.; Ghadiri, R.; Weigel, T.; Aumann, A.; Gurevich, E.; Esen, C.; Medenbach, O.; Cheng, W.; Chichkov, B.; Ostendorf, A. Comparison of in Situ and Ex Situ Methods for Synthesis of Two-Photon Polymerization Polymer Nanocomposites. *Polymers* 2014, 6 (7), 2037.
- [28] Hanemann, T.; Szabó, D. V. Polymer-Nanoparticle Composites: From Synthesis to Modern Applications. *Materials* 2010, 3 (6), 3468.
- [29] Kang, S. W. Role of p-Benzoquinone for Dispersion of Silver Nanoparticles in Silver-Polymer Nanocomposite Membranes. *Macromolecular Research* 2010, 18 (7), 705.
- [30] Fortunati, E.; Latterini, L.; Rinaldi, S.; Kenny, J. M.; Armentano, I. PLGA/Ag Nanocomposites: In Vitro Degradation Study and Silver Ion Release. *Journal of Materials Science: Materials in Medicine* 2011, 22 (12), 2735.
- [31] Lim, M. H.; Ast, D. G. Free-Standing Thin Films Containing Hexagonally Organized Silver Nanocrystals in a Polymer Matrix. *Advanced Materials* 2001, 13 (10), 718.

- [32] Prosycevas, I.; Puiso, J.; Guobiene, A.; Tamulevicius, S.; Naujokitis, R. Investigation of Silver Polymer Nanocomposites. *Material Science* 2007, 13 (3), 188.
- [33] Zeng, R.; Rong, M. Z.; Zhang, M. Q.; Liang, H. C.; Zeng, H. M. Laser Ablation of Polymer-Based Silver Nanocomposites. *Applied Surface Science* 2002, 187 (3), 239.
- [34] Hsu, S.; Tseng, H.-J.; Lin, Y.-C. The Biocompatibility and Antibacterial Properties of Waterborne Polyurethane-Silver Nanocomposites. *Biomaterials* 2010, 31 (26), 6796.
- [35] Vasiliev, A. N.; Gulliver, E. A.; Khinast, J. G.; Riman, R. E. Highly Dispersible Polymer-Coated Silver Nanoparticles. *Surface and Coatings Technology* 2009, 203 (19), 2841.
- [36] Carotenuto, G.; Pepe, G. P.; Nicolais, L. Preparation and Characterization of Nano-Sized Ag/PVP Composites for Optical Applications. *The European Physical Journal B* 2000, 16 (1), 11.
- [37] Abargues, R.; Rodriguez-Canto, P. J.; Albert, S.; Suarez, I.; Martínez-Pastor, J. P. Plasmonic Optical Sensors Printed from Ag–PVA Nanoinks. *Journal of Materials Chemistry C* 2014, 2 (5), 908.
- [38] Choudhury, A. Polyaniline/silver Nanocomposites: Dielectric Properties and Ethanol Vapour Sensitivity. *Sensors and Actuators B: Chemical* 2009, 138 (1), 318.
- [39] Lonjon, A.; Caffrey, I.; Carponcin, D.; Dantras, E.; Lacabanne, C. High Electrically Conductive Composites of Polyamide 11 Filled with Silver Nanowires: Nanocomposites Processing, Mechanical, and Electrical Analysis. *Journal of Non-Crystalline Solids* 2013, 376, 199.
- [40] Shah, M. S. A. S.; Nag, M.; Kalagara, T.; Singh, S.; Manorama, S. V. Silver on PEG-PU-TiO₂ Polymer Nanocomposite Films: An Excellent System for Antibacterial Applications. *Chemistry of Materials* 2008, 20 (7), 2455.

- [41] Kong, H.; Jang, J. One-Step Fabrication of Silver Nanoparticle Embedded Polymer Nanofibers by Radical-Mediated Dispersion Polymerization. *Chemical Communications* 2006, (28), 3010.
- [42] Dallas, P.; Sharma, V.; Zboril, R. Silver Polymeric Nanocomposites as Advanced Antimicrobial Agents: Classification, Synthetic Paths, Applications, and Perspectives. *Advances in Colloid and Interface Science* 2011, 166 (1-2), 119.
- [43] Sharma, V. K.; Yngard, R. A.; Lin, Y. Silver Nanoparticles: Green Synthesis and Their Antimicrobial Activities. *Advances in Colloid and Interface Science* 2009, 145 (1-2), 83.
- [44] Shameli, K.; Ahmad, M. B.; Yunus, W. M. Z. W.; Ibrahim, N. A.; Rahman, R. A.; Jokar, M.; Darroudi, M. Silver/poly(lactic acid) Nanocomposites: Preparation, Characterization, and Antibacterial Activity. *International Journal of Nanomedicine* 2010, 5, 573.
- [45] Egger, S.; Lehmann, R. P.; Height, M. J.; Loessner, M. J.; Schuppler, M. Antimicrobial Properties of a Novel Silver-Silica Nanocomposite Material. *Applied and Environmental Microbiology* 2009, 75 (9), 2973.
- [46] Love, J. C.; Estroff, L. A.; Kriebel, J. K.; Nuzzo, R. G.; Whitesides, G. M. Self-Assembled Monolayers of Thiolates on Metals as a Form of Nanotechnology. *Chemical Reviews* 2005, 36 (32), 1.
- [47] Ulman, A. Formation, and Structure of Self-Assembled Monolayers. *Chemical Reviews* 1996, 96 (4), 1533.
- [48] Toh, H. S.; Batchelor-McAuley, C.; Tschulik, K.; Compton, R. G. Chemical Interactions between Silver Nanoparticles and Thiols: A Comparison of Mercaptohexanol against Cysteine. *Science China Chemistry* 2014, 57 (9), 1199.

- [49] Manz, C.; Williams, L.; Mohseni, R.; Zlotnikov, E.; Vasiliev, A. Dispersibility of Organically Coated Silver Nanoparticles in Organic Media. *Colloids and Surfaces A: Physicochemical and Engineering Aspects* 2011, 385 (1-3), 201.
- [50] Bio-Rad/Sadtler IR Data Collection, Bio-Rad Laboratories, Philadelphia, PA (US).
- [51] Haken, J. K.; Werner, R. L. Infrared Spectrum of Polymethyl Acrylate. *British Polymer Journal* 1971, 3 (6), 263.
- [52] Finch, C. A. Proton and Carbon NMR Spectra of Polymers. *Polymer International* 1993, 31 (4), 403.
- [53] Fortier-McGill, B.; Toader, V.; Reven, L. ¹³C MAS NMR Study of Poly(methacrylic acid)–Polyether Complexes and Multilayers. *Macromolecules* 2014, 47 (13), 4298.
- [54] Speakman, S. Basics of X-Ray Powder Diffraction.
<http://prism.mit.edu/xray/oldsite/tutorials.htm> (accessed Mar 28, 2016).
- [55] Birks, L. S.; Friedman, H. Particle Size Determination from X-Ray Line Broadening. *Journal of Applied Physics* 1946, 17 (8), 687.
- [56] Goncalves, C.; Coutinho, J.; Marrucho, I. Optical Properties. In *Poly(lactic acid): Synthesis, structures, properties, processing, and applications* (Wiley Series on polymer engineering and technology); Lim, L.-T., Tsuji, H., Auras, R., Selke, S., Eds.; Wiley-Blackwell (an imprint of John Wiley & Sons Ltd): New Jersey, 2010; p 97.
- [57] Panáček, A.; Pucek, R.; Hrbáč, J.; Nevečná, T.; Šteffková, J.; Zbořil, R.; Kvítek, L. Polyacrylate-Assisted Size Control of Silver Nanoparticles and Their Catalytic Activity. *Chemistry of Materials* 2014, 26 (3), 1332.

- [58] Hua, F.; Kita, R.; Wegner, G.; Meyer, W. Interactions between Brushlike Polyacrylic Acid Side Chains on a Polyacrylate Backbone in Dioxane-Water. *ChemPhysChem* 2005, 6 (2), 336.
- [59] Kamyshny, A.; Ben-Moshe, M.; Aviezer, S.; Magdassi, S. Ink-Jet Printing of Metallic Nanoparticles and Microemulsions. *Macromolecular Rapid Communications* 2005, 26 (4), 281.
- [60] Magdassi, S.; Grouchko, M.; Berezin, O.; Kamyshny, A. Triggering the Sintering of Silver Nanoparticles at Room Temperature. *ACS Nano* 2010, 4 (4), 1943.
- [61] Long, Y.; Wu, J.; Wang, H.; Zhang, X.; Zhao, N.; Xu, J. Rapid Sintering of Silver Nanoparticles in an Electrolyte Solution at Room Temperature and Its Application to Fabricate Conductive Silver Films Using polydopamine as Adhesive Layers. *Journal of Materials Chemistry* 2011, 21 (13), 4875.
- [62] Ulrich, H. *Chemistry, and Technology of Carbodiimides*; Wiley and Sons: The United States, 2007.
- [63] Croll, T. I.; O'Connor, A. J.; Stevens, G. W.; Cooper-White, J. J. Controllable Surface Modification of Poly(lactic-co-glycolic acid) (PLGA) by Hydrolysis or Aminolysis I: Physical, Chemical, and Theoretical Aspects. *Biomacromolecules* 2004, 5 (2), 463.
- [64] Ashkarran, A.; Bayat, A. Surface Plasmon Resonance of Metal Nanostructures as a Complementary Technique for Microscopic Size Measurement. *International Nano Letters* 2013, 3 (1), 50.
- [65] Huang, T.; Xu, X.-H. N. Synthesis and Characterization of Tunable Rainbow Colored Colloidal Silver Nanoparticles Using Single-Nanoparticle Plasmonic Microscopy and Spectroscopy. *Journal of Materials Chemistry* 2010, 20 (44), 9867.

- [66] Karunamuni, R.; Maidment, A. D. A. Search for Novel Contrast Materials in Dual-Energy X-Ray Breast Imaging Using Theoretical Modeling of Contrast-to-Noise Ratio. *Physics in Medicine and Biology* 2014, 59 (15), 4311.
- [67] Panáček, A.; Kvítek, L.; Pucek, R.; Kolář, M.; Večeřová, R.; Pizúrová, N.; Sharma, V. K.; Nevěčná, T.; Zbořil, R. Silver Colloid Nanoparticles: Synthesis, Characterization, and Their Antibacterial Activity. *The Journal of Physical Chemistry B* 2006, 110 (33), 16248.
- [68] Choi, O.; Hu, Z. Size Dependent and Reactive Oxygen Species Related Nanosilver Toxicity to Nitrifying Bacteria. *Environmental Science & Technology* 2008, 42 (12), 4583.
- [69] Baker, C.; Pradhan, A.; Pakstis, L.; Pochan, D. J.; Shah, S. I. Synthesis and Antibacterial Properties of Silver Nanoparticles. *Journal of Nanoscience and Nanotechnology* 2005, 5 (2), 244.

VITA

ANITA PAUL

Education:

B.Sc. Chemistry, University of Bombay, India (May 1989).
Applied Components Groups - Chemistry, Drugs, and Dyes

Diploma in Industrial Analytical Chemistry,
University of Bombay, India (1990)

Diploma in Systems Management in National Institute of
Information Technology-NIIT (1995)

M.S. Chemistry East Tennessee State University, Johnson City, TN
(August 2016)

Research Advisor: Dr. Aleksey Vasiliev, Silver-Polymer
Nanocomposites

Professional Experience:

May & Baker Limited, Mumbai, India (January – February '90)
Trainee Analyst
Responsibilities included: Analysis of raw materials and finished
products.

ANA Laboratories, Mumbai, India (April 1991 – February 1992)
Analytical Chemist
Responsibilities included: Analysis of chemicals in the Chemical and
Instrumentation Division.

GUFIC Limited, Mumbai, India (March 1992 – August 1995)
Administrative Assistant
Responsibilities included: Administration for Medical Sales
representatives

Computation Services, Mumbai, India (September – November
1995)
Computer Programmer
Responsibilities included: Programming in COBOL

Publications:

J. Ellison, G. Wykoff, A. Paul, R. Mohseni, A. Vasiliev. Efficient dispersion of coated silver nanoparticles in the polymer matrix. *Colloids and Surfaces A: Physicochemical and Engineering Aspects* 2014, v. 447, p. 67-70.

A. Paul, E. Kaverina, A. Vasiliev. Synthesis of silver-polymer nanocomposites by surface coating, using carbodiimide method. *Colloids and Surfaces A: Physicochemical and Engineering Aspects* 2015, v. 482, p. 44-49.

Presentations:

J. Ellison, G. Wykoff, A. Paul, R. Mohseni, A. Vasiliev. Silver-Polymer nanocomposite material. 247th ACS National Meeting, March 16-20, 2014, Dallas, TX. COLL-141.

A. Paul, J. Ellison, A. Vasiliev. Novel Ag-poly(methylacrylate) nanocomposite materials. 2014 Appalachian Student Research Forum, April 2-3, 2014, Johnson City, TN.

A. Vasiliev, A. Paul. Biodegradable polymer materials containing stabilized silver nanoparticles. 249th ACS National Meeting, March 22-26, 2015, Denver, CO. COLL-125.

A. Paul, A. Vasiliev. Biodegradable X-ray contrast nanomaterials. 2015 Appalachian Student Research Forum, April 8-9, 2015, Johnson City, TN.